International Journal of Coal Geology 286 (2024) 104507

Contents lists available at ScienceDirect

International Journal of Coal Geology

journal homepage: www.elsevier.com/locate/coal

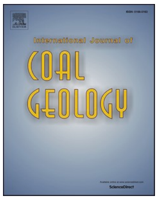

Petrology and organic geochemistry of the Middle Devonian cutinitic liptobioliths from Luquan region, Yunnan Province, China

Daofu Song [a,*], Tieguan Wang [a], Hao Wang [a], Honghe Xu [b], Zhengang Lu [a], Yue Liu [a]

[a] State Key Laboratory of Petroleum Resources and Engineering, China University of Petroleum, Beijing 102249, China
[b] State Key Laboratory of Palaeobiology and Stratigraphy, Nanjing Institute of Geology and Palaeontology, Chinese Academy of Sciences, Nanjing 210008, China

ARTICLE INFO

Keywords:
Liptobiolith
Coal chemistry
Macerals
Molecular composition
Coal-forming plants
Cutinite enrichment

ABSTRACT

The majority of Middle Devonian coal samples from Wujing (WJ), Damo (DM), and Batang (BT) areas in the Luquan region of China have cutinite content exceeding 50%, classifying them as typical cutinitic liptobioliths. These coals are notable for their thinly-bedded texture, which allows them to split readily into leaf-like laminae. However, coals from these areas display distinct macroscopic, microscopic, and geochemical features. The split laminae from WJ and DM coals are black and ribbon-like, with those from WJ being notably longer and wider. In contrast, BT coal laminae are irregular, small fragments with golden or brown hues. Correspondingly, the cutinite in WJ coals is predominantly thick-walled, DM coals primarily contain a medium-walled type, and BT coals are characterized by a thin-walled type. Additionally, BT coals are rich in sporinite, with some classified as sporinite-rich durain or sporinitic liptobiolith. Abundant tetracyclic diterpenoids were detected in the maltene fraction of all the coal extracts. The concentration and composition of these diterpenoids are influenced by the content and type of cutinite present in the coals. The presence of tetracyclic diterpenoids, with beyerane, atisane and kaurane skeletons, had already evolved in early land plants. This implies that the precursors of these compounds were likely significant components of the cuticles of early land plants or, at least coexisted alongside plant cuticles. The spore assemblages in coals and the microscopic features of cutinite suggest that the coal-forming plants of the Luquan cutinitic liptobioliths were early land plants, predominantly herbaceous lycopsids, rhyniopsids, *Orestovia* and *Spongiophyton*. However, it is important to note that the specific types of these coal-forming plants may vary by areas. This variation leads to the distinctive macroscopic and microscopic characteristics observed in coals from different locations.

Cutinitic liptobiolith appears to have been exclusive to the Middle Devonian period, especially during the Givetian. The emergence of this distinct coal type is likely due to the unique structure of Devonian land plants. Specifically, the combination of well-developed cuticles and less developed woody tissues in these early land plants might have played a key role in the formation of cutinitic liptobioliths.

1. Introduction

Coals with over 50% liptinite (on a mineral matter-free basis) are called liptobioliths, while those rich in liptinite but with <50% liptinite are classified as liptinite-rich durain (Han et al., 1996). Cutinitic liptobioliths, characterized by a predominant cutinite content (>50% on a mineral matter-free basis), are rare and found in only a few locations worldwide, such as China, Siberia, Kazakhstan, Timan and Germany (Ammosov, 1964; Han, 1964; Sheng et al., 1991; Volkova, 1994; Dai et al., 2006; Song et al., 2017, 2021, 2022a). These unique coals, often referred to as "paper coals' or "leaf coals", exhibit a distinctive foliated, papery texture when weathered. This type of coal seems to be specific for the Middle Devonian (Kashirtsev et al., 2010; Song et al., 2022a), as most reported instances of such coal occurred during Givetian, despite limited peat accumulation during this period. Devonian cutinitic liptobioliths have attracted considerable interest due to their unique petrography, geochemistry, coal-forming plants, and oil-prone potential, and their significance in marking the beginning of coal formation in geological history (Dai et al., 2006).

In China, Han (1964) first described a Devonian cutinitic liptobiolith from the Luquan region, located on the east side of the Kangdian Uplift (Fig. 1), making the Luquan coal internationally renowned.

---

* Corresponding author.
E-mail address: songdaofu2008@163.com (D. Song).

https://doi.org/10.1016/j.coal.2024.104507
Received 8 February 2024; Received in revised form 27 March 2024; Accepted 28 March 2024

Subsequently, the Luquan paper coals garnered significant interest from researchers and were widely studied (Han, 1989; Sheng et al., 1991; Han et al., 1993, 1996; Cheng et al., 1995; Dai et al., 2006). Han et al. (1993, 1996) and Cheng et al. (1995) provided detailed summaries of their quality and petrographic characteristics, suggesting that they are typical cutinitic liptobiolith with cutinite content >60% and sporinite content <10%. However, Dai et al. (2006) investigated some Devonian coals from the Luquan region and found that these coals have high contents of cutinite and sporinite (27.4–83.2% and 7–71%, respectively, on a mineral matter-free basis). As a result, they classified these Luquan coals as cutinitic liptobiolith, sporinite-rich durain, sporinitic liptobiolith, and cutinite-rich durain. The distinctive maceral compositions reported by different researchers may be attributed to their samples originating from various areas within the Luquan region. In fact, the Middle Devonian liptobioliths were deposited in three locations in the Luquan region, including Wujing, Batang and Damo areas. It is noteworthy that the samples from these different locations not only have variable maceral compositions but also possess distinct petrological and geochemical features. In this paper, samples were collected from Wujing, Batang and Damo areas, and their petrology, geochemistry, coal-forming plants, and peat accumulation conditions were studied in detail.

2. Geological setting

The Luquan region, located at the southwestern margin of the Yangtze Block, experienced significant geological changes during the Late Ordovician period as a result of the Caledonian Orogeny. This tectonic activity led to a substantial uplift and land expansion from the Silurian into the Early Devonian (Han, 1989). By the late Early Devonian, the region began to accumulate new sedimentary deposits due to the subsidence of the regional basement. These deposits, primarily composed of terrestrial sandstones, shales and conglomerates, were confined to a relatively limited area. Up to the Middle Devonian, a marked transgression occurred in a northeasterly direction across South China, resulting in the extensive deposition of coastal sediments in the study area (Fig. 1a). However, during the late Devonian period, a brief phase of geological uplift occurred, leading to the absence of Upper Devonian strata in the geological record (Fang, 2000).

Middle Devonian strata in this region are assigned to the Yuzidian and Haikou Formations (Fig. 2; Fang, 2000). The Yuzidian Formation, positioned at the base of the Middle Devonian, is about 50 m thick. It primarily comprised thin-bedded sandstones and yellow-gray shales, intercalated with oolitic hematite deposit. Above it, the upper Haikou Formation, which varies in thickness from 380 to 450 m, is composed mainly of clastic rocks deposited in a shallow marine environment. This includes layers of purplish gray shale, grayish white fine-grained sandstone, purple shales, mudstones, coal beds, gray shales, and siltstones, with intercalated dolomite and limestone. Notably, some clastic rocks, characteristic of the littoral facies, are found at the base of this formation (Han, 1989; Dai et al., 2006). The geological period of the Haikou Formation is believed to be the early Givetian of the Middle Devonian based on spore assemblages and reginal correlation (Han et al., 1996; Wang et al., 2007; Marshall et al., 2017). Additionally, the cutinitic liptobiolith is found within the formation.

3. Samples and methods

Fifteen Devonian coal samples were collected from outcrops in the Luquan region (Fig. 1b), including five samples from the Wujing area (identified as WJ-1 to WJ-5), five samples from the Damo area (DM-1 to DM-5) and five samples from the Batang area (BT-1 to BT-5). All five samples from each area were collected from the same outcrop. Due to the thinness of the coal beds, ranging from 0.1 to 0.5 m, the samples were collected randomly but were carefully selected to represent different segments of these slender coal layers. To avoid the effects of weathering, a trench perpendicular to the strike of the coal streak was dug in each area. Representative bulk samples of the Devonian coals were taken from the trench. Subsequently, the samples were immediately sealed in paper bags to minimize contamination. In the lab, the outer surfaces were removed to further prevent contamination, and then the bulk samples were crushed into pieces smaller than 1 cm in size. The freshest pieces were handpicked for subsequent analysis.

The coal blocks for microscopic examination (perpendicular to bedding) were ground and polished on a Buehler automatic machine (EcoMet 250 with AutoMet 250). Maceral analyses were determined under a Leica DMRXP microscope using incident white light and bule-light excitation. Maceral classification and terminology in this study adhere to the ICCP System1994 (International Committee for Coal and

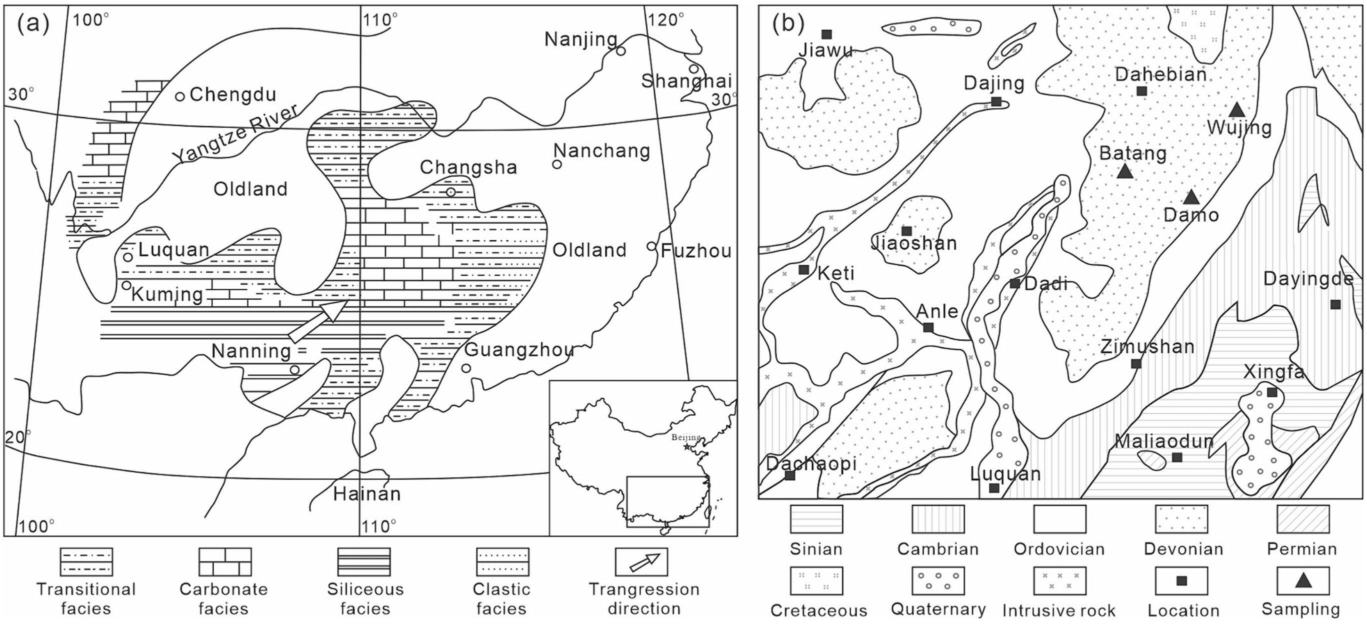

Fig. 1. The Middle Devonian paleogeographic map of south China (a, modified after Han, 1989) and the geological map of the Luquan area showing the sample location (b).

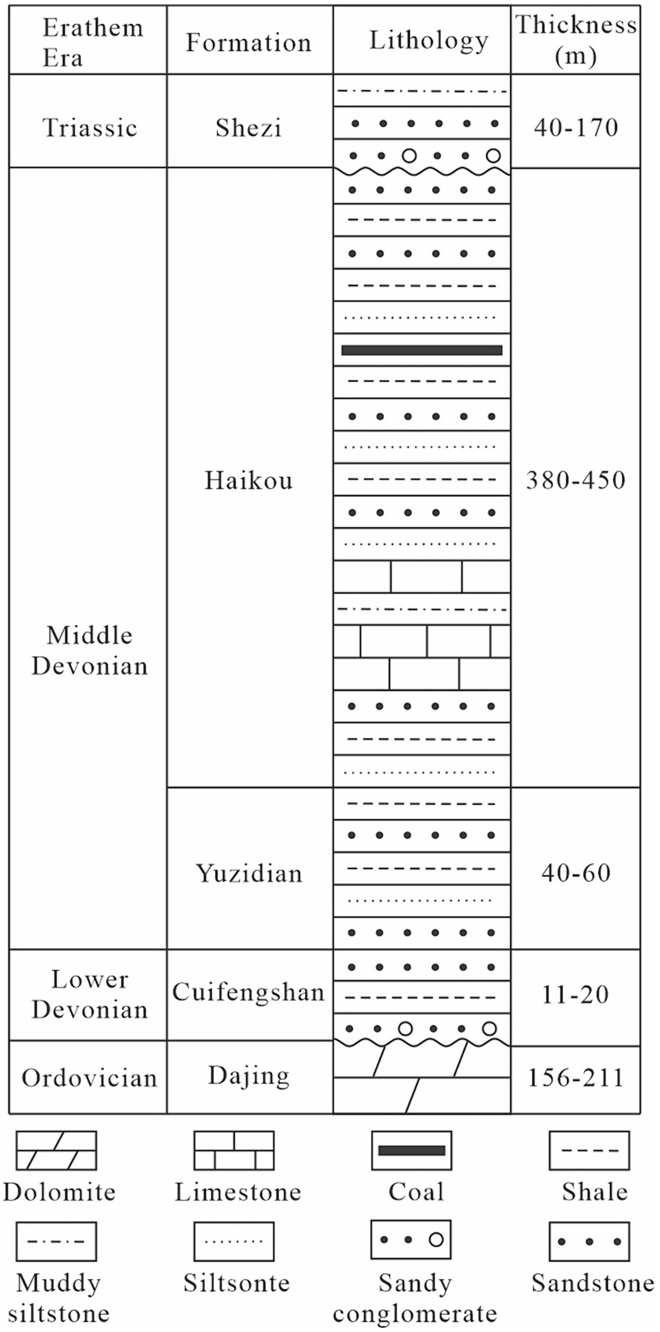

Fig. 2. Generalized stratigraphy of the Luquan region (Fang, 2000).

Organic Petrology (ICCP), 1998; International Committee for Coal and Organic Petrology (ICCP), 2001) and Pickel et al. (2017). Vitrinite reflectance was measured following ASTM Standard D2798-11a (2019) using a Leica DM4500P microscope with a CRAIC microscope photometer, after calibration against the saphir standard (Ro =0.589%). To further reveal the detailed microscopic characteristics, selected sample blocks were coated with gold and then examined with a field emission-scanning electron microscope (SEM).

Proximate analysis was performed in accordance with ASTM Standard D3173 (2011), ASTM Standard D3174 (2011), and ASTM Standard D3175 (2011). Total sulfur contents were determined following ASTM Standard D3177-02 (2011). Ultimate analyses (C, H, O, and N contents) were performed using a Vario Macro Elemental Analyzer. Total organic carbon (TOC) content was determined using a Leco CS-230 analyzer. For this measurement, 12.5% HCl was added into the ground sample to remove carbonates, and then the sample was washed with distilled water for three days. Rock pyrolysis measurements were conducted using a Rock-Eval 6 instrument. The pyrolysis temperature was programmed from an initial temperature of 300 °C (held for 3 min) to a final temperature of 600 °C at 50 °C/min. The free hydrocarbon (S_1) peak is achieved during thermal heating at 300 °C, whereas the hydrocarbons generated from pyrolysis from 300 °C to 600 °C were defined as the residual hydrocarbons (S_2) fraction.

For chemical analysis, the fresh samples were powdered and Soxhlet extracted for 24 h with a dichloromethane/methanol mixture (2:1). The extracts were deasphalted using *n*-hexane, and separated using column chromatography (silica gel over alumina, 3:1) into saturate, aromatic, and NSO fractions by sequential elution with *n*-hexane, toluene, and dichloromethane/methanol mixture (2:1). Before gas chromatography analysis, the silylation of the NSO fraction was accomplished using BSTFA+TMCS (99/1). Gas chromatography–mass spectrometry (GC–MS) analyses of the saturated, aromatic, and NSO fractions were conducted using an Agilent Model 6890 gas chromatograph coupled to an Agilent Model 5975i mass selective detector, and fitted with a HP-5MS capillary column (60 m, 0.25 mm i.d., 0.25 μm film thickness). The GC operating conditions for the saturated and NSO fractions were: 50 °C (1 min) to 120 °C at 20 °C/min, and then to 260 °C at 2 °C/min (hold for 25 min); for the aromatic fraction were: 80 °C (1 min) to 310 °C at 3 °C/min (hold for 25 min). The MS transfer line temperature was held at 280 °C and the ion source temperature was 250 °C. The sample was injected in a splitless mode, with an injector temperature at 300 °C. The ion source was operated in the electron impact (EI) ionization mode at 70 eV. Helium was used as the carrier gas (flow rate 1.0 ml/min).

Reference standards of phyllocladanes and kauranes were obtained by catalytic hydrogenation of the natural products phyllocladene and kaurene. Reduction of phyllocladene yielded 16α(H)- and 16β(H)-phyllocladane in a ratio of 4:1 and similarly for kaurene, with the GC elution order of β before a for both sets of standards, as previously reported (Noble et al., 1985, 1986). The yielded phyllocladanes and kauranes were analyzed by GC–MS as external standards. Identification of individual diterpene in the coal samples was based on a comparison of the mass spectra and the relative GC retention times with the external standards and those previously reported. Quantitative results of diterpanes and *n*-alkanes were achieved by peak area integration using phyllocladene and n-$C_{24}D_{50}$ as internal standards, respectively.

The palynological analysis involved standard HCl-HF-HCl palynological maceration techniques, beginning with an initial treatment in 30% HCl followed by decant washing in water until pH neutral. Subsequently, demineralization in 60% HF with repeated stirring was performed. The organic residues were sieved through a 10 μm mesh and concentrated by heavy liquid separation using a zinc bromide solution (2.0 g/cm^3). Afterward, the residues were mounted in hydroxyethyl cellulose and sealed with synthetic resin. Spores were observed and photographed using a Zeiss AX10 microscope.

4. Results

4.1. Macroscopic characteristics

The Devonian coals in the Luquan region occur as lenticular bodies, typically with a thickness of 0.1–0.5 m, and in some areas exceeding 1.0 m. These coals appear dark gray or black color on their fresh surfaces, while their weathered surfaces often appear yellowish-brown or buff. They are dull coals, displaying a dull or resinous luster. All of the Devonian coals are characterized by a distinct papery texture (Fig. 3), giving them the appearance of a stack of paper sheets, which has earned them the nickname “paper coal” (Han, 1989). These coals can be easily split into leaf-like laminae with good elastic property, which separate during weathering. However, the split laminae of the coals from different areas exhibit distinct macroscopic characteristics (Fig. 3). The laminae in both the WJ and DM coal samples are characterized by a

Fig. 3. Macroscopic characteristics of the Devonian cutinitic liptobiolith from the WJ (a, b), DM (c, d) and BT areas (e, f).

black, ribbon-like appearance. However, there is a significant difference in size between them. The laminae from WJ coal are generally larger, typically measuring 1.0–2.0 cm in width and 10–20 cm in length. In contrast, the laminae from DM coals are smaller, with dimensions of about 0.5–1.0 cm in width and <5 cm in length (Fig. 3b, d). The laminae in the BT coal samples are markedly different from those of WJ and DM coals, primarily appearing as irregular small fragments and exhibit a golden or brown color (Fig. 3f). These variations in macroscopic characteristics are also reflected in their distinct maceral composition.

4.2. Coal chemistry and vitrinite reflectance

Table 1 summarizes the results of proximate and ultimate analyses, as well as these of the determinations of total sulfur content, caloric value, random vitrinite reflectance, and pyrolysis for the cutinitic liptobioliths. The moisture (air-dry basis) in all the samples is low, ranging from 1.68% to 3.62% with an average of 2.30%. The ash yield (dry basis) for the WJ liptobioliths varies from 6.63% to 15.00%, classifying them as low-medium ash coal according to ISO classification 11,760 (2005). In contrast, the ash yield for the DM (24.80–36.36%) and BT liptobioliths (33.29–35.12%) is much higher, making them moderately high to high ash coals. The total organic carbon (TOC, air-dry basis) content for the WJ, DM, and BT cutinitic liptobioliths is 59.63–65.87%, 47.63–54.51%, 47.4–49.74%, respectively, showing an apparent negative correlation with ash yields. The volatile matter yield (dry and ash-free basis) and the gross calorific values (on moist, ash-free basis) in all the samples (64.92–81.74% and 23.03–33.46 MJ/kg, respectively) indicate a high volatile subbituminous to bituminous rank according to ASTM Standard D388 (2018). However, the volatile matter yield in the cutinitic liptobioliths is much higher than expected for a common bituminous coal, which can be attributed to the elevated cutinite content (Song et al., 2022a). In addition, the accumulation of cutinite also results in high hydrogen content in the liptobioliths (8.60–9.14%, daf), which is much higher than that of typical type-III kerogen. The H/C and O/C ratios for the analyzed coals are 1.45–1.52 and 0.14–0.18, respectively, indicating a type-II kerogen (Fig. 4a, Mukhopadhyay et al., 1991). This

Table 1
Results of proximate and ultimate analyses, total sulfur content, caloric value, TOC and Rock-Eval pyrolysis, as well as maximum vitrinite reflectance data.

Sample no.	Location	Proximate analysis				Ultimate analysis						TOC and Rock-Eval pyrolysis analysis					$Q_{ad, af}$ MJ/kg	Rr (%)
		M_{ad} (%)	A_d (%)	V_{daf} (%)	FC_{daf} (%)	C_{daf} (%)	H_{daf} (%)	O_{daf} (%)	N_{daf} (%)	H/C	O/C	TOC (%)	S_1 mg/g	S_2 mg/g	HI mg/g·TOC	Tmax °C		
WJ-1	Wujing	2.47	6.63	80.68	19.32	71.65	8.70	17.32	0.34	1.46	0.18	65.87	30.22	339.33	515.15	439	32.10	0.52
WJ-2		2.28	11.50	79.76	20.24	71.73	9.09	16.54	0.30	1.52	0.17	62.28	30.21	314.73	505.35	442	32.58	0.54
WJ-3		2.53	12.99	80.99	19.01	71.62	8.70	17.13	0.31	1.46	0.18	59.63	21.61	304.10	509.98	440	31.77	0.52
WJ-4		2.25	6.57	81.74	18.26	71.29	8.65	17.24	0.34	1.46	0.18	63.46	26.87	321.17	506.10	441	33.46	0.55
WJ-5		2.60	15.00	78.18	21.82	71.43	9.05	16.47	0.30	1.52	0.17	58.41	22.39	297.58	509.47	442	30.83	0.56
DM-1	Damo	2.03	24.80	75.53	24.47	69.75	8.77	15.75	0.25	1.51	0.17	54.51	11.57	256.24	470.08	440	26.98	0.40
DM-2		2.05	25.99	75.17	24.83	68.45	8.6	16.58	0.20	1.51	0.18	52.71	17.42	285.52	541.68	438	23.03	0.39
DM-3		2.85	31.17	81.74	18.26	68.77	8.71	16.17	0.23	1.52	0.18	47.83	12.91	260.91	545.49	437	26.02	0.39
DM-4		3.18	31.30	71.78	28.22	69.38	8.72	15.67	0.25	1.51	0.17	48.54	12.39	257.58	530.66	438	25.78	0.40
DM-5		3.62	36.36	70.66	29.34	68.17	8.56	16.51	0.20	1.51	0.18	47.63	11.61	234.01	491.31	438	23.48	0.39
BT-1	Batang	1.78	33.29	74.29	25.71	75.10	9.14	14.24	0.27	1.46	0.14	48.90	9.96	251.99	515.32	435	26.94	0.36
BT-2		1.68	33.33	74.47	25.53	74.08	9.05	14.39	0.30	1.47	0.15	49.74	12.90	258.74	520.18	433	27.46	0.35
BT-3		1.68	34.10	64.92	35.08	75.23	9.11	14.32	0.29	1.45	0.14	48.41	12.39	257.58	532.08	436	27.68	0.36
BT-4		1.68	35.12	70.98	29.02	73.68	8.97	13.97	0.26	1.46	0.14	47.42	9.91	243.72	513.96	435	26.44	0.36
BT-5		1.84	34.34	71.16	28.84	72.11	8.81	14.01	0.29	1.47	0.15	48.52	12.62	253.03	521.50	435	27.54	0.36

M, moisture; A, ash yield; V, volatile matter; FC, fixed carbon; Qgr, gross calorific value; C, carbon; H, hydrogen; O, oxygen; N, nitrogen; ad, air-dry basis; d, dry basis; af, ash-free basis; daf, dry and ash-free basis, TOC, total organic carbon content; HI, hydrogen index.

Note: The sum of C + H + O + N is not 100% due to the presence of sulfur and other minor organic elements.

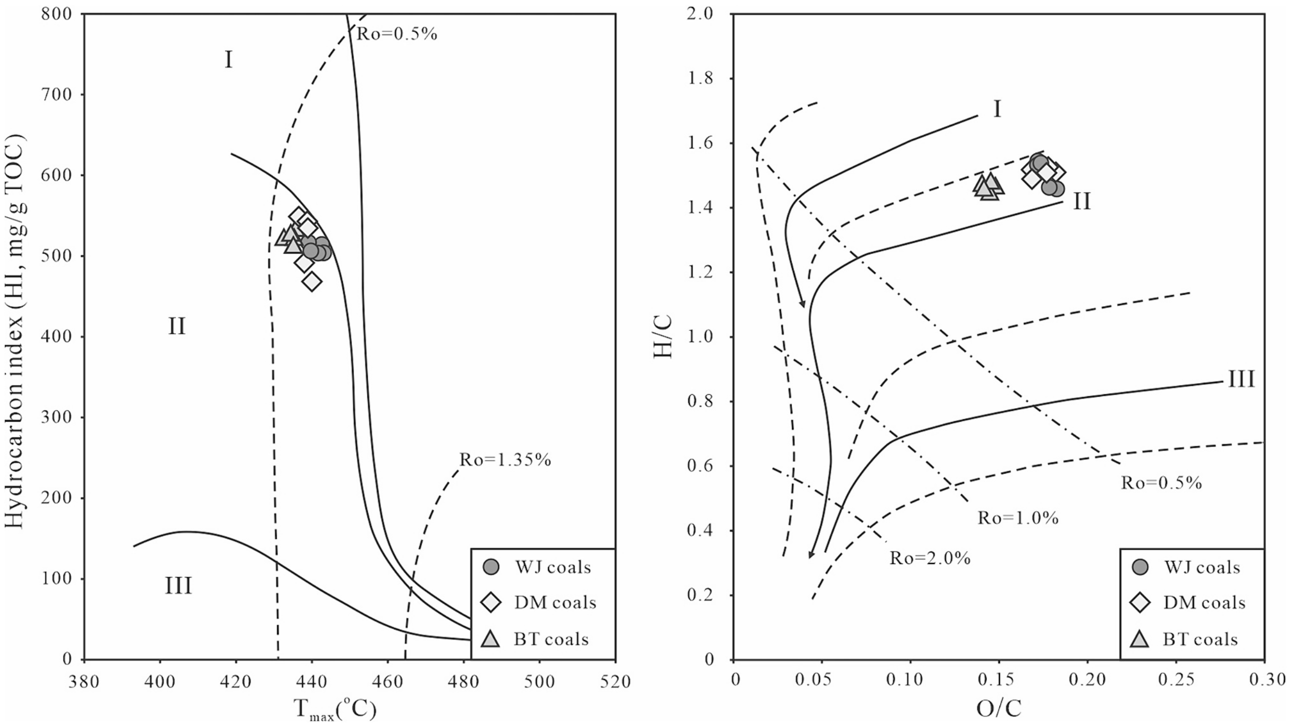

Fig. 4. Plots of T_{max} vs. HI (a) and O/C vs. H/C (b) indicating the kerogen types of the Luquan liptobioliths.

result is also confirmed by the pyrolysis parameters of HI and T_{max} values (Fig. 4b, Van Krevelen, 1961). The extremely high volatile matter yield, and very high S_2 and HI values suggest an excellent oil generation potential for these cutinitic liptobioliths.

The measured random vitrinite reflectance values for the WJ coals range from 0.52% to 0.56%, consistent with previous findings (Sheng et al., 1991; Han et al., 1993; Cheng et al., 1995). In contrast, the DM and BT coals have lower values of 0.39–0.40% and 0.35–0.36%, respectively, indicating a lower thermal maturity. T_{max} values, a common index of organic matter maturation (Tissot and Welte, 1984; Peters and Moldowan, 1993), range from 439 to 442 °C for the WJ coals, from 437 to 440 °C for the DM coals, and from 433 to 436 °C for the BT coals. Using the conversion relationship of $Rc = 0.013 \times T_{max} - 5.0$ (Evenick, 2021), the calculated Rc values for the WJ, DM and BT coals are 0.71–0.75%, 0.68–0.72%, and 0.63–0.67%, respectively. The Rc values for all the coals are much higher than their measured vitrinite reflectance, likely indicating a strong suppression of vitrinite reflectance. This is not surprising for cutinitic liptobioliths, as vitrinite surrounded by abundant hydrogen-rich macerals (e.g., cutinite, sporinite and alginite) tends have a suppressed reflectance (Kalkreuth, 1982; Peterson and Vosgeran, 1999). Furthermore, the collodetrinite macerals in the BT coals exhibit a weak fluorescence, indicating they are perhydrous. Perhydrous collodetrinite typically has lower reflectance values compared to normal vitrinite.

Given the suppression of vitrinite reflectance in our samples, coal rank determination is more appropriately based on calculated Rc values. In summary, the majority of the examined samples can be classified as high volatile bituminous coals, based on their Rc values, volatile matter yields, and calorific values, in accordance with ASTM Standard D388 (2018) and ISO 11760 (2005) standards. Notably, Devonian liptobioliths from the Baishaping, Panzhihua, and northwest Xinjiang regions within China exhibit characteristics akin to our findings, especially an unusually high volatile matter yield and comparable coal ranks, as documented by Song et al. (2022a, 2022b). Additionally, Volkova (1994) has identified similar coal ranks and properties in Devonian liptobioliths from the Bazas region in Russia.

4.3. Microscopic characteristics

The majority of the analyzed Devonian Luquan coals are typical cutinitic liptobioliths, with a cutinite content of >50% (Han et al., 1996). However, the coals from different areas vary in cutinite type, microstructure, and maceral composition. These differences are likely attributable to the distinct flora, paleoenvironment, and coal-forming conditions in each area.

In WJ coals, sections perpendicular to the bedding commonly display alternating thick ribbon-like cutinite and narrower bands of vitrinite under the microscope (Fig. 5). Clayey partings observed between these macerals cause the coal to easily split into laminae during weathering. Each separated lamina consists of two cutinite slices on both sides and one collodetrinite slice in the middle (Fig. 5c, d), representing a cross-section through a ribbon-like stem. Occasionally, the ribbon-like cutinite is arranged in parallel, directly on top of one another. According to Han et al. (1996), cutinite can be classified into three types based on width: thin-walled (<5 μm), medium-walled (10-50 μm) and thick-walled cutinite (>50 μm). In WJ coals, thick-walled cutinite (50–500 μm wide) is most dominant, with smaller amounts of medium-walled and thin-walled types (Han et al., 1996). The contents of these cutinite types are 61.5–70.1% for thick-walled, 1.1–2.9% for medium-walled, and 1.0–2.1% for thin-walled cutinite. Characteristically, all these types of cutinite have a smooth outer edge and display a brilliant yellow fluorescence.

The vitrinite in WJ liptobioliths is primarily composed of telinite (2.4–4.6%) and collodetrinite (14.1–16.8%, Table 2). Collodetrinite typically appears as a structureless, homogeneous mass in a ribbon-like shape and often exhibits a fragmentary nature due to desiccation cracks, which can be filled with exsudatinite (Fig. 5d). Exsudatinite, characterized as expelled hydrocarbon liberated from the lipid constituents of liptinite macerals, marks the first coalification jump and beginning of bituminization (Teichmiiller, 1974; Teichmtiller, 1974). Inertinite is present in small amount in WJ coals, including fusinite, macrinite, micinite and inertodetrinite. Along with minor quantities of sporinite and liptodetrinite, these inertinite components are primarily dispersed in the clayey partings. Fusinite is characterized by a well-preserved

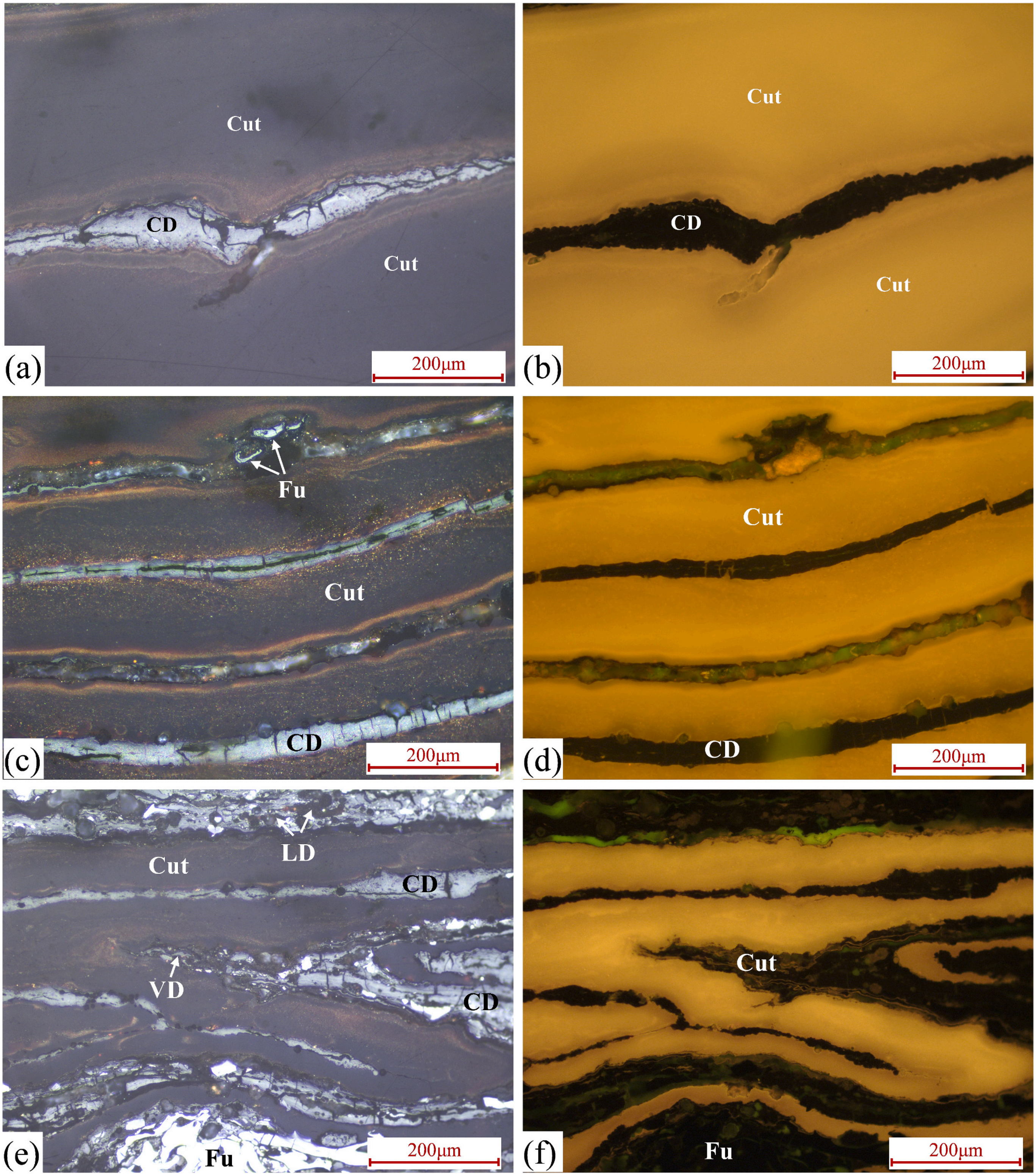

Fig. 5. Photomicrographs of the WJ Devonian cutinitic liptobioliths (a, c, e-under incident white light and oil immersion; b, d, f-in fluorescence mode). Cut, cutinite; CD, collodetrinite; Fu, fusinite; LD, liptodetrinite; VD, vitrodetrinite.

cellular structure, exhibiting a white color under incident white light with high reflectance and relief. However, in many cases, the walls of the empty cells have been fractured and pushed into one another, creating bogen or star structures. These fusinite fragments are typically scattered in the clayey partings or assembled together as lenticles or impersistent layers. The fusinite may have originated from forest fires or incomplete combustion, either occurring in situ or windblown into peat swamps (Scot and Glasspool, 2007; Diessel, 2010; Moroeng et al., 2018).

In DM coals, medium-walled cutinite represents the predominant type, accounting for average content of 84.22%, while thin-walled cutinite is less common, comprising an average content of 12.84% (Fig. 6; Table 2). Both types typically exhibit a brown color under

Table 2
Maceral composition of the Luquan cutinitic liptobiolihts.

Sample no.	Location	Maceral composition (vol%; on mineral matter-free basis)												
		Cut			Sp	Ex	LD	T	CD	VD	F	Mac	Mic	ID
		Thick-walled	Medium-walled	Thin-walled										
WJ-1	Wujing	65.1	2.6	1.7	0.8	0.8	3.4	4.2	14.3	0.3	3.8	1.6	0.2	1.2
WJ-2		66.3	2.9	1.8	0.9	0.5	0.7	4.6	14.7	0.4	3.8	2.3	0.2	0.9
WJ-3		70.1	2	1.0	0.9	0.5	5.6	2.4	14.1	0.2	2.3	0	0.4	0.5
WJ-4		62.8	1.8	2.1	1.2	0.3	1.2	3.8	15.7	0.2	7.6	1.8	0.3	1.2
WJ-5		61.5	1.1	1.5	1.5	0.6	3.8	4.6	16.8	0.3	5.8	0.9	0.5	1.1
DM-1	Damo	–	82	14.9	1.3	–	0.5	–	0.7	–	–	0.6	–	–
DM-2		–	81.5	15.2	1.5	–	0.3	–	1.4	–	–	–	–	0.1
DM-3		–	75.7	21.6	1.3	–	0.2	–	1	–	–	–	–	0.2
DM-4		–	92.3	5.3	0.8	–	0.4	–	1.1	–	0.1	–	–	–
DM-5		–	89.6	7.2	1.1	–	0.5	–	1.3	–	0.1	–	0.1	0.1
BT-1	Batang	–	–	54.6	43.9	–	0.1	–	1.4	–	–	–	–	–
BT-2		–	0.2	52.4	43.9	–	–	–	3.5	–	–	–	–	–
BT-3		–	–	45.8	51.8	–	–	–	2.4	–	–	–	–	–
BT-4		–	0.1	54.8	43.1	–	0.2	–	1.8	–	–	–	–	–
BT-5		–	–	43.2	55.1	–	0.1	–	1.5	–	0.1	–	–	–

Cut, cutinite; Sp, sporinite; Ex, exsudatinite; LD, liptodetrinite; T, telinite; CD, collodetrinite; VD, vitrodetrinite; F, fusinite; Mac, macrinite; Mic, macrinite; ID, inertodetrinite.

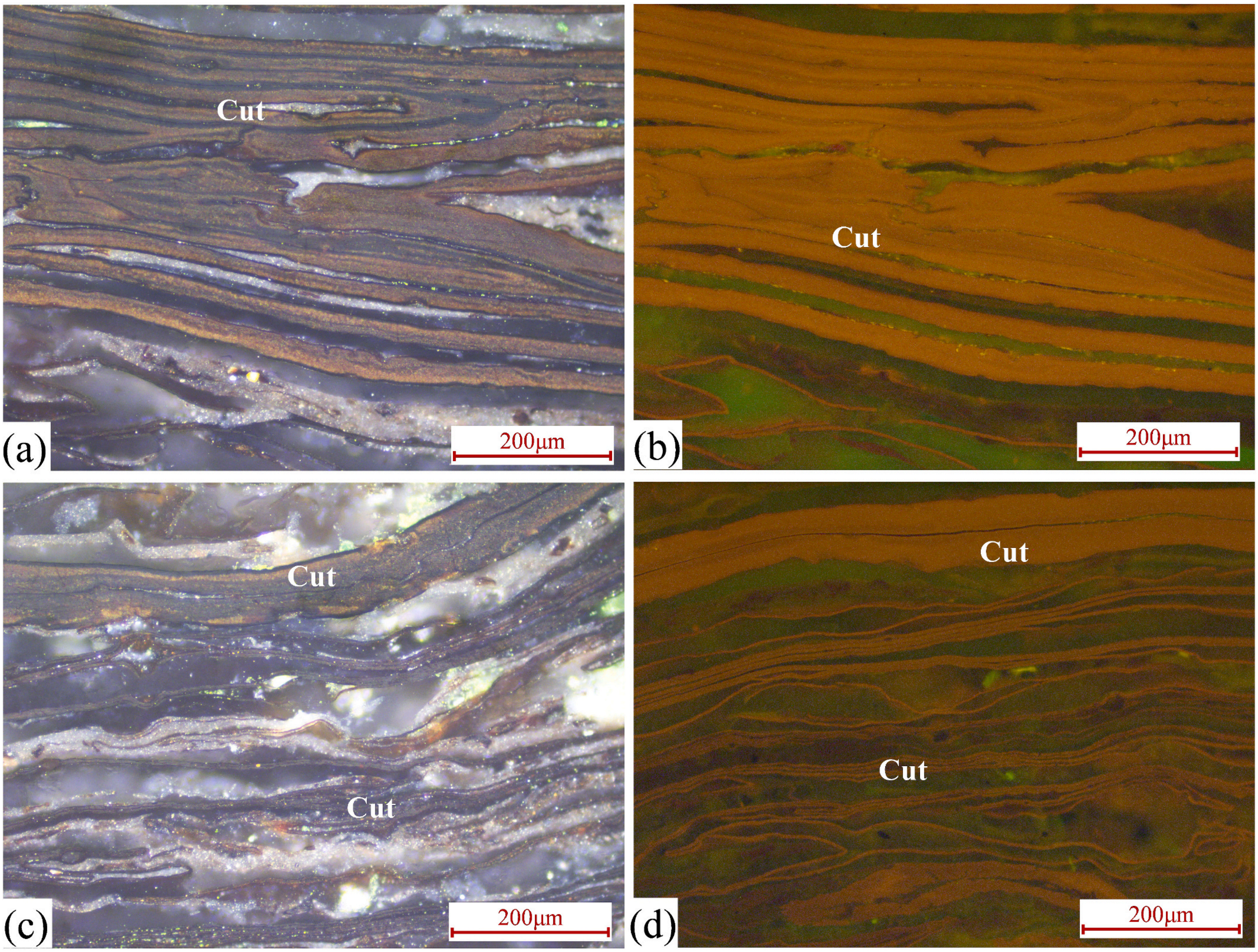

Fig. 6. Photomicrographs of the DM cutinitic liptobioliths (a, c- under incident white light and oil immersion; b, d-in fluorescence mode). Cut, cutinite.

incident while light and a weak brown color in fluorescence mode, suggesting intense weathering. However, they differ in their physical features: medium-walled cutinite often has either serrated or smooth edges, whereas thin-walled cutinite typically features smooth edges. Additionally, sporinite is primarily dispersed within the clayey partings, with an average content of 1.2%. Other macerals in DM coals, such as vitrinite and inertinite, are found in trace amounts.

In BT coals, cutinite is exclusively thin-walled, with widths typically ranging from 1 to 5 μm, and displays a bright yellow color under blue-light excitation (Fig. 7). The content of thin-walled cutinite in these coals varies from 43.2% to 54.8%, with an average of 50.16%. Additionally, BT coals are rich in sporinite, predominantly composed of microsporinite. The microsporinite has lengths ranging from 15 μm to 100 μm, commonly between 20 and 60 μm, and a wall thickness generally between 1 and 3 μm, though occasionally up to 10 μm (Fig. 7). Morphologically, microsporinite in BT coals is often disc-shaped, elliptical or elongated thread-like bodies, sometimes featuring serrated outer edges. It appears dark gray under incident while light and exhibit a weak

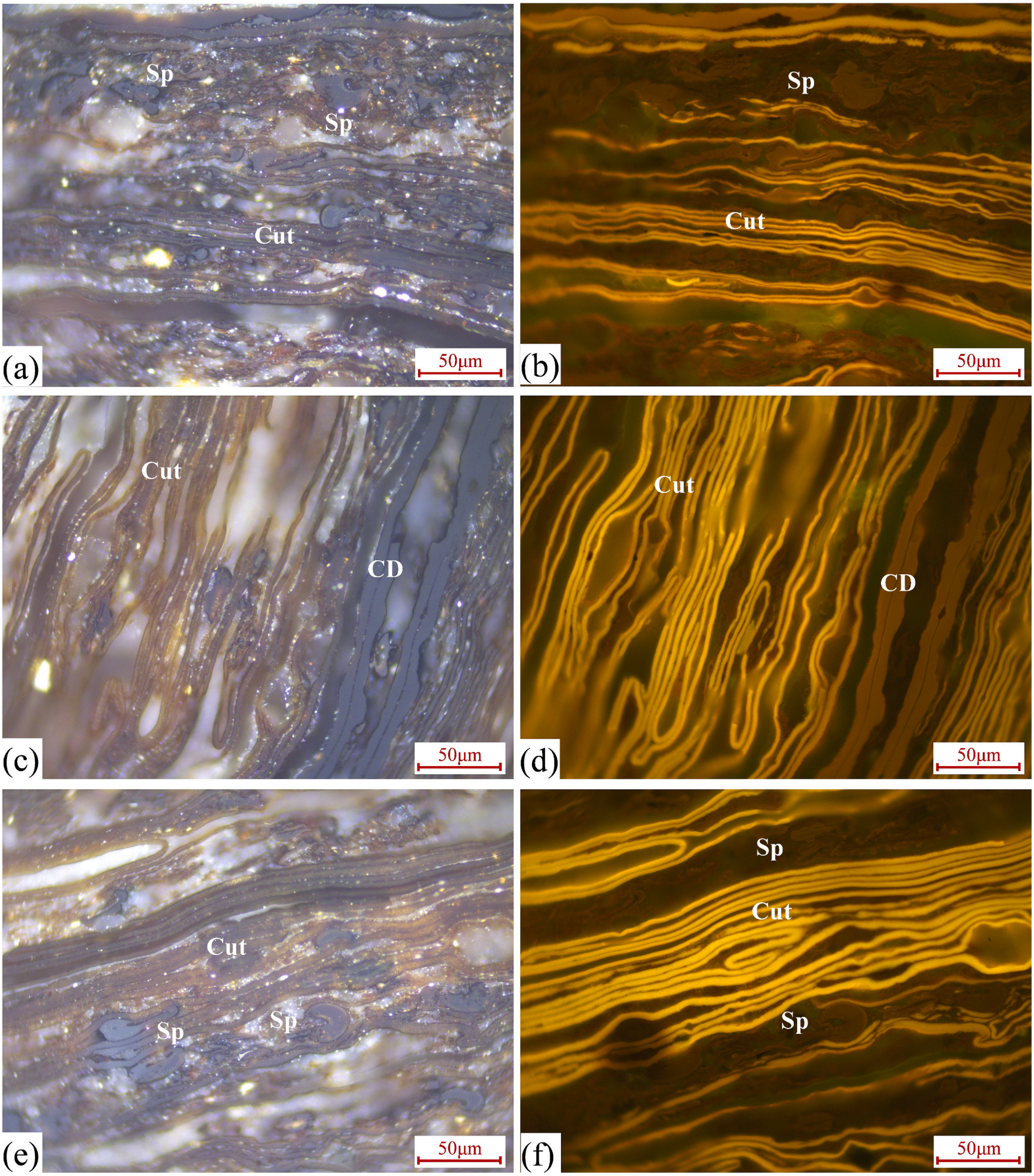

Fig. 7. Photomicrographs of the BT Devonian cutinitic liptobioliths (a, c, e-under incident white light and oil immersion; b, d, f-in fluorescence mode). Cut, cutinite; CD, collodetrinite; Sp, sporinite.

brown color under blue-light excitation. The sporinite content in BT coals ranges from 43.1% to 55.1%, with an average of 47.56%. As a result, BT coals can be classified as cutinitic liptobiolith, sporinite-rich durain, sporinitic liptobiolith, or cutinite-rich durain. The maceral composition of BT liptobioliths is largely similar to the Luquan liptobioliths described by Dai et al. (2006). Vitrinite and inertinite are found only in trace amounts within BT coals. The vitrinite is primarily collodetrinite, typically displaying a weak brown fluorescence, indicative of a perhydrous type (Fig. 7d).

Differences among cutinite macerals are evident not only in their width but also in their microscopic features. Notably, thick and medium-walled cutinite is characterized by numerous small pores (<1 μm), randomly distributed within the cutinite (Fig. 8a). Conversely, thin-walled cutinite exhibits a more uniform and homogeneous structure (Fig. 8b). Additionally, distinctive features such as stomata and tubercles are frequently observed on the surface of thick or medium-walled cutinite. The stomata observed on these cutinite macerals are typically elliptical or semirounded and are randomly distributed on the surface (Fig. 8c, d). These stomata have sizes ranging from 100 to 200 μm in length and 50–120 μm in width, with each flanked by two reniform guard cells (kindey-shaped). The tubercles on the cutinite macerals also exhibit a variation in diameter, ranging from 50 to 100 μm, and display various shapes such as conoidal, spiniform, and dome-shaped (Fig. 8e, f). Intriguingly, these tubercles develop central canals and are believed

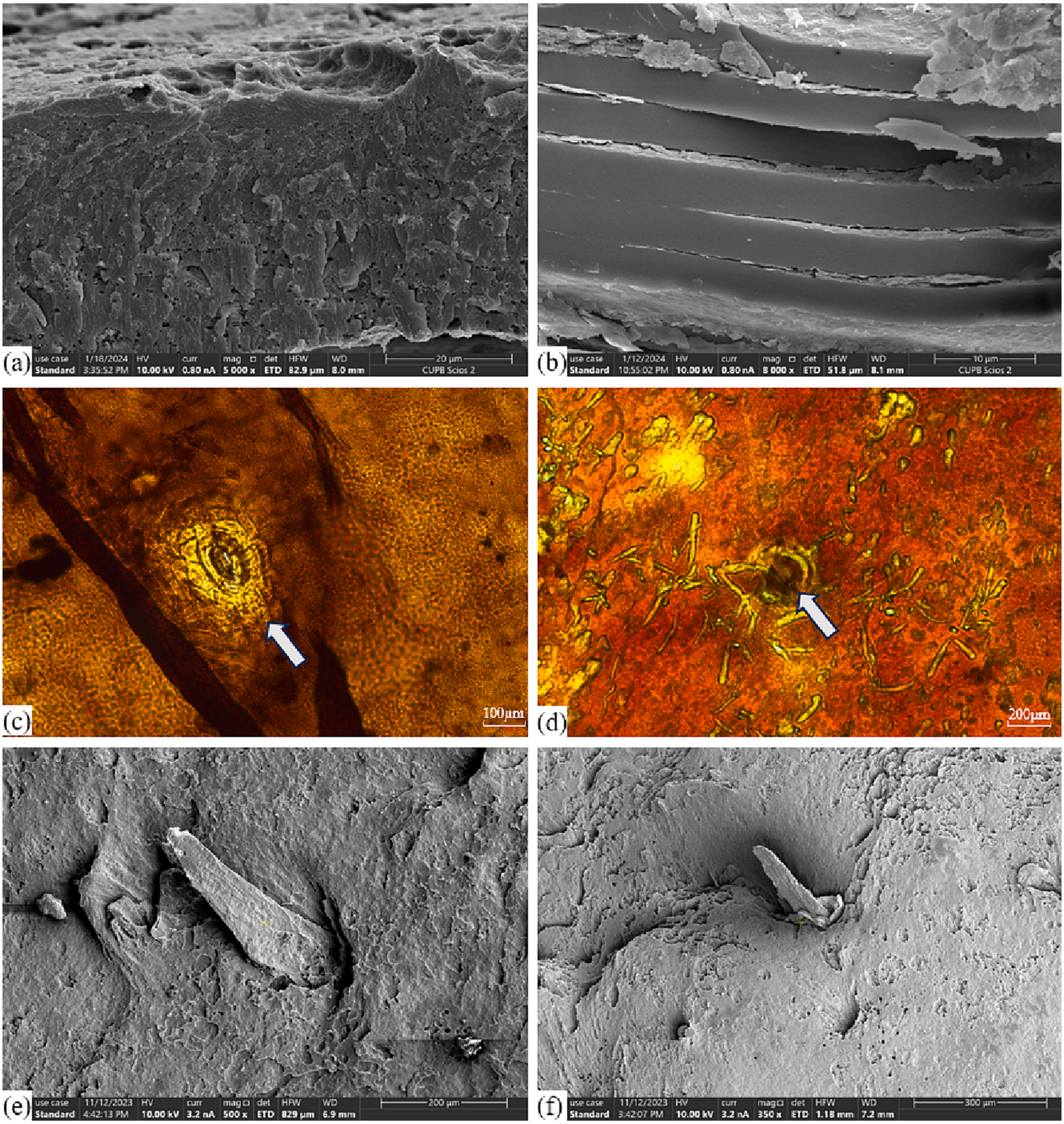

Fig. 8. Microscopic characteristics of the Luquan Devonian cutinitic liptobioliths (a, b, e, f-SEM back-scattered image; c, d -in transmitted light). (a) Medium-walled cutinite featuring numberous small pores, (b) thin-walled cutinite with a uniform and homogeneous structure, (c-d) various shapes of stomata, (e-f) tubercles present on the surface of cutinite.

to have a secretory function (Krassilov, 1981).

4.4. Organic geochemistry

As shown in Fig. 9, the saturate fraction of Luquan cutinitic liptobioliths primarily consists of *n*-alkanes and tetracyclic diterpanes. Long chain alkanes (C_{23}-C_{27}) dominate in WJ and BT coals, while DM coals contain a higher abundance of short-chain homologues. It remains unclear if the high abundance of short-chain n-alkanes in DM coals is syngenetic to the coals or originates from modern organisms during weathering. In all samples, long-chain *n*-alkanes display an apparent odd predominance, with CPI values >1.0. These *n*-alkanes typically originate from cuticular waxes, either synthesized directly by higher plants or defunctionalized from even-numbered acids, alcohols, or esters (Tissot and Welte, 1984; Peters et al., 2005). Notably, nC_{25} and nC_{27} alkanes in all samples are present in much higher abundance relative to their adjacent homologues. In the lower-matured BT coals, the abundance of nC_{25} and nC_{27} alkanes is more than double that of their adjacent homologues. Pristane (Pr) is present only in trace amounts, while phytane is below the detection limit. The most abundant source of Pr and Ph is the phytyl side chain of chlorophyll *a* in phototrophic organisms (Powell and McKirdy, 1973). Consequently, these compounds are typically found in high abundance in the low-moderate matured sediments, particularly coals. The absence of Pr and Ph in the Devonian coals from Luquan region warrants further investigation.

Tetracyclic diterpanes are highly abundant in the saturated fractions of Devonian coals. These compounds, which have a general formula of C_nH_{2n-6}, elute between nC_{18} and nC_{24} on the TIC trace. C_{20} tetracyclic diterpanes and their C_{20+} homologues mainly exhibit base peaks at *m/z* 123. In contrast, C_{19} and C_{18} terpanes typically show base peaks at *m/z* 231 and 245, which are characteristic of tetracyclic norditerpanes (Sheng et al., 1992). In the Devonian coal samples, the most abundant

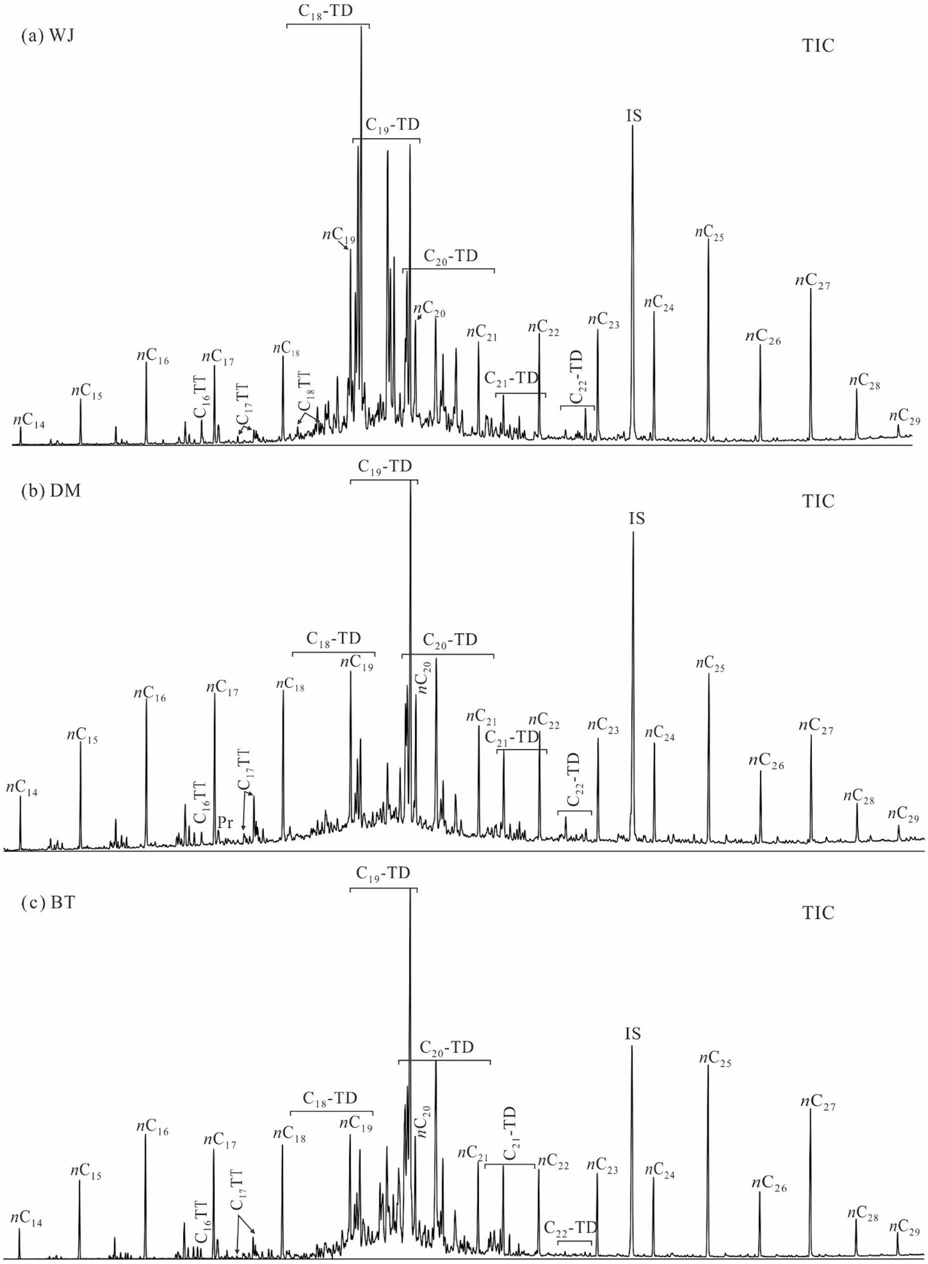

Fig. 9. Representative saturate fraction gas chromatograms of the WJ (a), DM (b) and BT (c) cutinitic liptobioliths. *n*, normal alkanes; C_i, carbon number; IS, internal standard; TT, tricyclic terpanes; TD, tetracyclic diterpanes.

constituents are C_{20} tetracyclic diterpanes and their C_{18}–C_{19} homologues. These compounds include well-known types like beyeranes, kauranes, phyllocladanes, and atisanes. In the analyzed samples, however, the number of C_{20} tetracyclic diterpane isomers and their homologues is much greater than previously reported (Fig. 10). Some of these compounds can be identified up to C_{36}, albeit in lower abundance.

In this study, some tetracyclic diterpanes with relatively high abundances were carefully identified by comparing their GC retention times and mass spectra with external standards and previous reports (Fig. 11; Noble et al., 1985, 1986; Song et al., 2017, 2022a). These diterpanes labeled 1a to 3 g in Fig. 10, can be classified as follows: diterpane 1a is a C_{18} bisnor-tetracyclic diterpane; diterpane 2a-2f are C_{19} demethylated tetracyclic diterpanes; and diterpane 3a-3 g are C_{20} homologues. Diterpane 3a, eluting earlier than other isomers, is identified as beyerane due to its base peak at *m/z* 123 and a prominent key ion at *m/z* 245. Diterpane 3b is identified as either 16β(H)-atisane or 16β(H)-kaurane, based on its base peak at *m/z* 123 and key ions at *m/z* 231 and 259. Atisane has both 16α(H)- and 16β(H)-stereoisomers, with the latter typically co-eluting with 16β(H)-kaurane under standard GC–MS conditions (Peters et al., 2005). The *m/z* 231/259 ratio, a diagnostic indicator to distinguish kauranes/atisanes from phyllocladanes, is <0.3 for diterpane 3b, indicative of kauranes or atisanes (Noble et al., 1985; Mei et al., 1989). Diterpane 3d is identified as 16α(H)-atisane based on its retention time and mass spectra, featuring major ions at *m/z* 123, 189, 231 and 259. Typically, 16β(H) tetracyclic diterpanes are more abundant than their 16α(H) counterparts in sedimentary organic matter

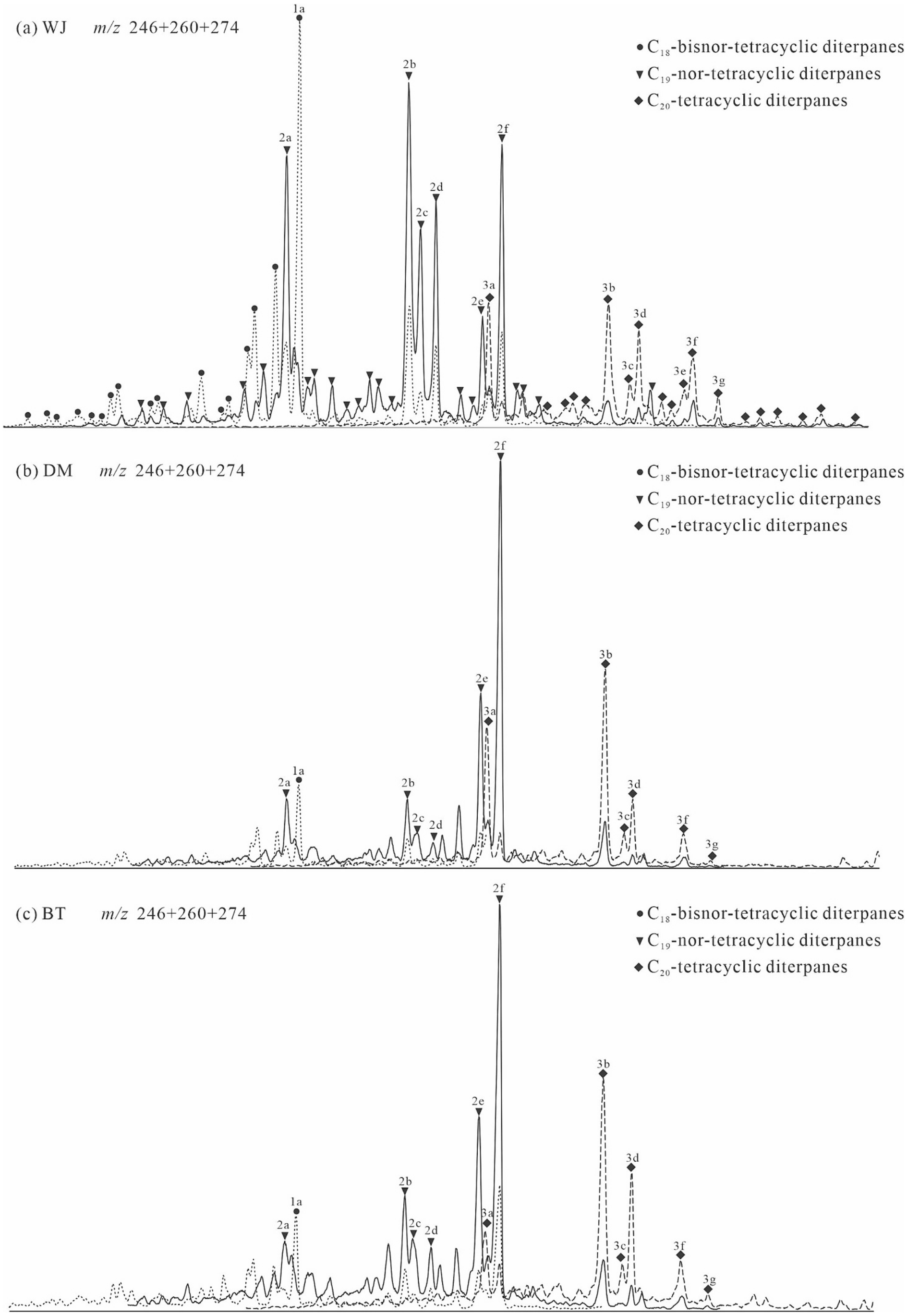

Fig. 10. Representative saturate fraction *m/z* 246, 260 and 274 chromatograms showing the C_{18}-C_{20} tetracyclic diterpane distribution in the WJ (a), DM (b) and BT (c) cutinitic liptobioliths.

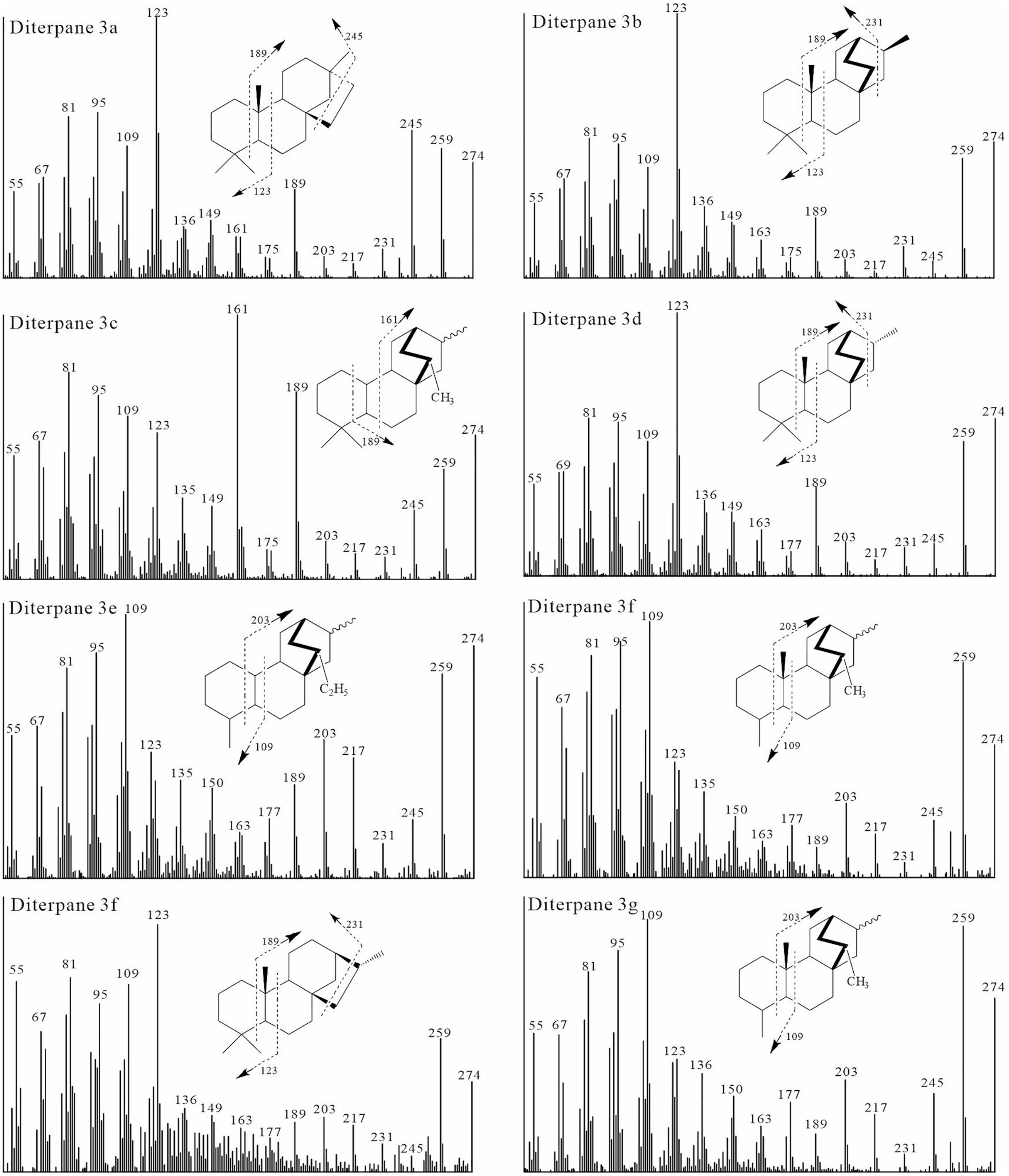

Fig. 11. Mass spectra for the diterpanes 3a-3 g labeled in Fig. 9.

due to greater stability during catagenesis. The higher abundance of 16α (H)-atisane in Luquan coals suggests diterpane 3b is primarily 16β(H)-atisane. Diterpane 3c, tentatively identified as 20-normethylatisane, has a mass spectrum with major ions at *m/z* 161, 189, 245 and 259, which differs from known tetracyclic diterpanes like phyllocladane or kaurane (Noble et al., 1985, 1986; Peters et al., 2005; Zinniker, 2005). Diterpane 3e exhibits a significant *m/z* 109 ion, indicating its A-ring fragment has one less methylene unit than beyerane, atisane or kaurane (Noble et al., 1985). The increased abundance of *m/z* 203 suggests that diterpane 3e has a methyl substituent on either ring C or D, making its mass spectrum best fit for 19,20-bisnorethylatisane. Diterpane 3f is a mixture of two co-eluted compounds. In the BT and DM coals, diterpane 3f has a base peak at m/z 123 and is identified as 16α(H)-kaurane based on its retention time and mass spectra. In the WJ coals, however, diterpane 3f displays a base peak at m/z 109 and key ions at 123, 203, 217 and 259, leading to its identification as 19-normethylatisane. Thus, diterpane 3f consists of 16α(H)-kaurane and co-eluted 19-normethylatisane, with the former being predominant in BT and DM coals and the latter being dominant in WJ coals. Lastly, Diterpane 3 g has a base peak at m/z 109 and key ions at 123, 203, 217 and 259, identifying it as 19-normethylatisane. Considering the high abundance and stability of atisane, the mass spectra of most other compounds were interpreted as being based on the atisane skeleton. As a result, diterpane 1a has been identified as 17,19-bisnoratisane. Similarly, diterpane 2a to 2f have been identified as 19-norbeyerane, 19-norkaurane, 19,20-bisnormethylatisane, 19-noratisane and 17-noratisane, respectively.

In addition to the tetracyclic diterpanes, a high abundance of C_{18}-C_{19} tetracyclic diterpenones was detected in the WJ and DM Middle Devonian cutinitic liptobioliths (Fig. 12). However, these compounds were either absent or only present in low abundance in the BT coal samples. As expected, C_{16} and C_{18} fatty acids, which are the primary constituents of cutin, were detected in all the NSO fractions.

4.5. *Coal-forming plants*

Extensive research has been conducted on the coal-forming plants of the Luquan Devonian cutinitic liptobioliths. Psilopsids and lycopsids, the dominant terrestrial plants during the Middle Devonian age, are believed to be the main contributors to the formation of these special coal deposits (Sheng et al., 1992; Dai et al., 2006).

In this study, terrestrial spores present in the samples were extensively analyzed to identify the plants contributing to coal formation (Fig. 13). The palynoflora of the WJ coals is dominated by *Ancyrospora*, accounting for 33.3% of the total spore flora (Table 3). Although the specific species of *Ancyrospora* remains uncertain, it is evident that the plants producing *Ancyrospora* spores were major contributors to the coal formation. The WJ palynoflora also includes significant proportions of rhyniophytes (18.9%), herbaceous lycopsids (21.3%), and sphenospids (9.8%). In contrast, the DM and BT coal samples have a higher prevalence of herbaceous lycopsid spores (Fig. 14). These spores constitute a remarkable 94.0% of the palynoflora in DM coals, where other spore types are relatively rare. In the BT coals, lycopsid spores make up 32.5% of the palynoflora, accompanied by notable amounts of rhyniophyte (24.4%), sphenopsid (5.2%), and filicale (15.5%) spores.

The microscopic characteristics of cutinite, notably the stomata and cuticle structure, are key indicators of their origins. According to Guo and Wang (2016), the stomata observed on Luquan cutinite can be classified into rosette and complex types. The rosette-type stomata (Fig. 8d) are commonly found in Devonian rhyniopsids, zosterophyllopsids, lycopsids, and a progymnosperms. In contrast, the complex type of stomata (Fig. 8c), exclusive to the Middle Devonian, is likely associated with *Orestovia*. Furthermore, the cutinite observed in WJ and DM coals, characterized by thick and medium walls with oval to circular pores, is reminiscent of those found in the Lower-Middle Devonian *Spongiophyton*. Initially, *Spongiophyton* was proposed as a terrestrial evolutionary intermediate between algae and vascular land plants (Gensel et al., 1991). Later, it was reidentified as a lichen because of an internal cortex of fungal hyphae (Stein et al., 1993) and stable carbon isotope data (Jahren et al., 2003). However, the lichen affinities of *Spongiophyton* were questioned by Fletcher et al. (2004), adding complexity to its classification.

Based on the analysis of spore assemblages and the microscopic characteristics of cutinite, it is possible to conclude that the coal-forming plants of the Luquan cutinitic liptobioliths were early land plants, mainly including herbaceous lycopsids, rhyniopsids, *Orestovia*, and *Spongiophyton*. However, it is important to note that the specific types of these coal-forming plants can vary by area. This variation leads to the distinctive macroscopic and microscopic characteristics observed in coals from different locations. Generally, the WJ coals, characterized by a predominance of thick-walled cutinite, are likely to have a higher contribution from *Spongiophyton*. In contrast, the DM and BT coals, dominated by medium to thin-walled cutinite, may have a greater input from lycopsids, because *Cymbosporites* are dominant spores in these coals.

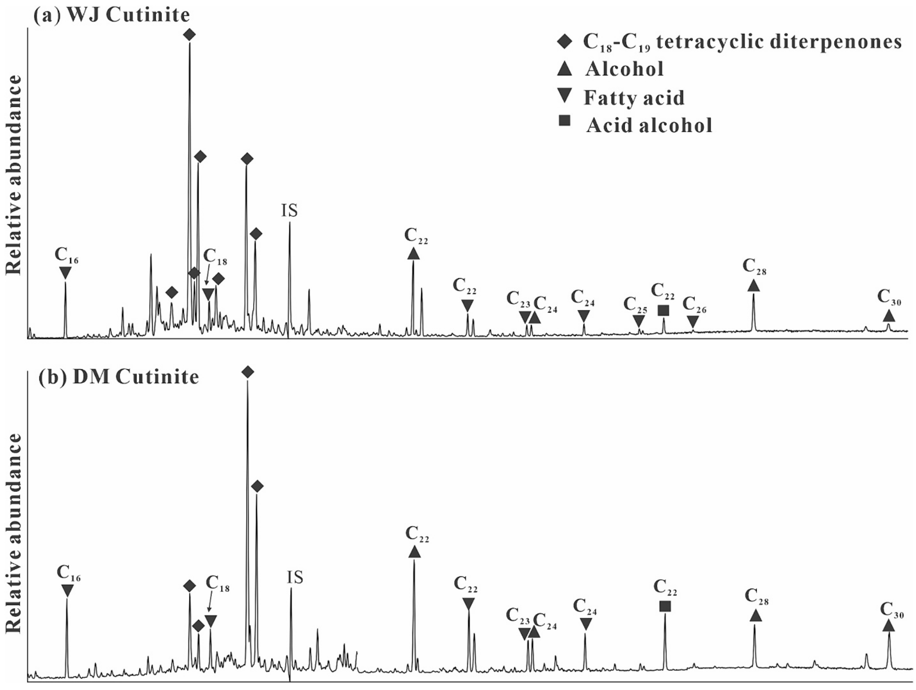

Fig. 12. Representative NSO fraction gas chromatograms of the WJ (a) and DM (b) cutinitic liptobioliths.

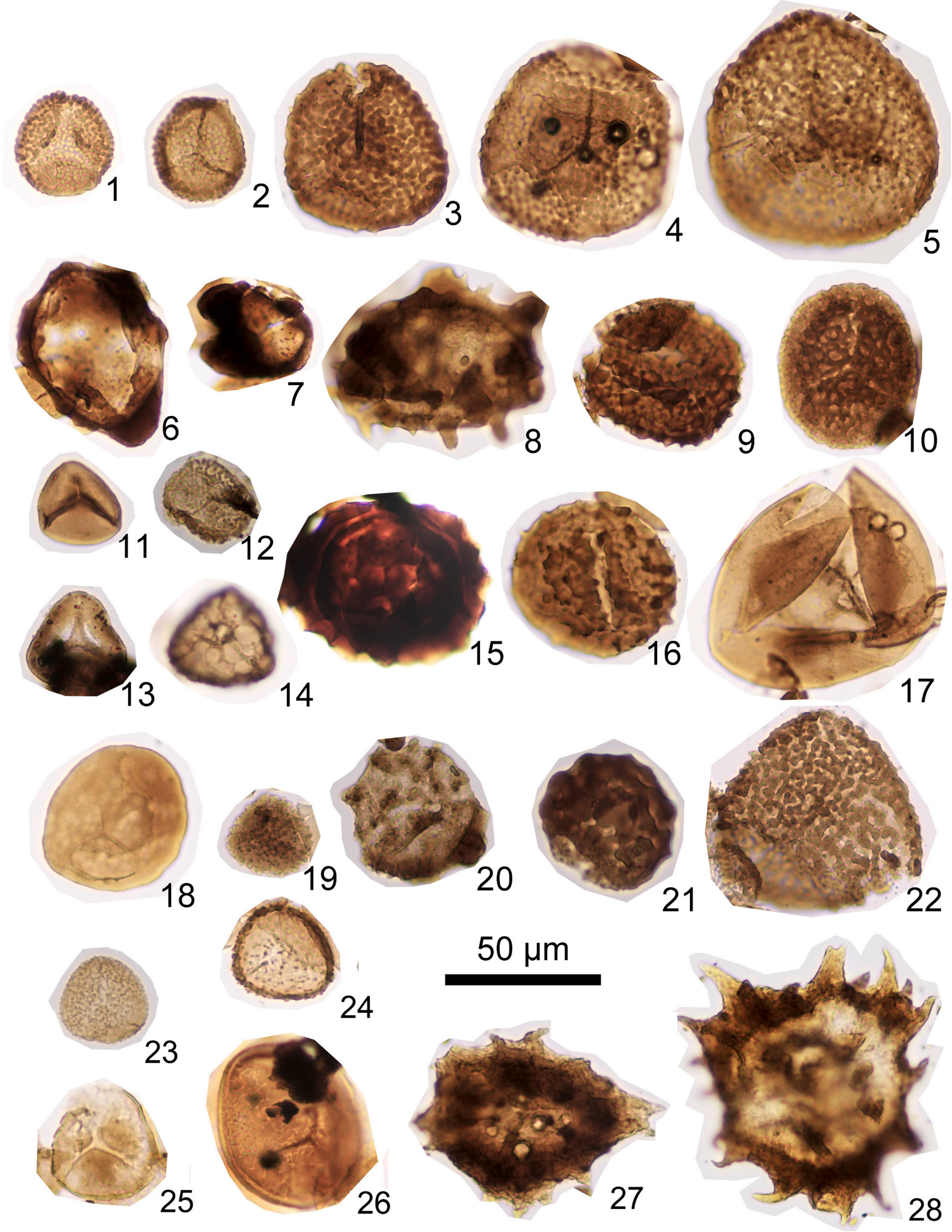

Fig. 13. Various palynomorphs observed in the Luquan coals. 1–2. *Cymbosporites microverrucosus*; 3. Cymbosporites coniformis; 4. Cymbosporites conatus; 5. Cymbosporites pallida; 6. Lophozonotriletes verrucosus; 7. Lophozonotriletes irregularis; 8. Lophozonotriletes baculiformis; 9. Camptotriletes sp.; 10–11. Retusotriletes sp.; 12. Apiculiretusispora sp.; 13. Leiotriletes sp.; 14. Dictyotriletes sp.; 15. Chelinospora sp.; 16. Thymospora imperfecta; 17. Calamospora sp.; 18. Archaeozonetriletes sp.; 19. Lophotriletes trivialis; 20. Lophotriletes rarus; 21. Brochotriletes sp.; 22. Acinosporites sp.; 23. Granulatisporites sp.; 24. Cymbosporites sp.; 25. Retusotriletes biarelis; 26. Punctatisporites sp.; 27. Ancyrospora incisa; 28. Ancyrospora sp.

Table 3
Quantitative palynological characteristics of the studied samples (percentage, Balme, 1995).

Parent plant	Spores	WJ coals	DM coals	BT coals
Rhyniophytes	*Retusotriletes triangulatus*			2.6
	R. biarelis		0.5	
	R. sp.	13.1	0.5	8.7
	Apiculiretusispora sp.	5.8		13.1
Sphenopsids	*Calamospora* sp.	9.8	0.5	5.2
Filicales	*Punctatisporites* sp.	2.5		
	Raistrickia levis			0.4
	R. sp.		0.5	1.7
	Thymospora imperfecta			0.4
	Leiotriletes sp.	1.7	0.5	1.7
	Planisporites sp.			0.4
	Lophotriletes rarus			2.6
	L. sp.			0.9
	Apiculatisporis sp.	0.8		
	Cyclogranisporites			0.4
	Convolutispora sp.		0.5	0.9
	Camptotriletess sp.			1.3
	Dictyotriletes sp.		0.5	3.9
	Granulatisporites sp.		0.5	0.9
Herbaceous lycopsids	*Cymbosporites conatus*	13.4	89.2	19.2
	C. microverrucosus	3.1	4.8	10.2
	C. coniformis			0.4
	C. pallida			0.9
	C. sp.	4.8		1.8
Gymnosperm	*Monocolpates*			0.4
Unknow	*Crissisporites* sp.			2.6
	Anapiculatisportes dilutus	0.7		
	Brochotriletes sp.			0.4
	Archaeozonotriletes splendidus	0.7		
	A. irregularis	0.7		
	A. sp.	1.5		1.3
	Acinosporites sp.			3.0
	Tholisporites sp.	0.8		
	Chelinospora robusta		0.5	0.4
	C. sp.	2.2	0.5	4.3
	Lophozonotriletes baculiformis			1.7
	L. verrucosus		0.5	0.9
	L. irregularis			0.4
	L. sp.	5.1	0.5	7.0
	Ancyrospora incisa	11.6		
	A. arquta	3.6		
	A. simplex	14.5		
	A. sp.	3.6		

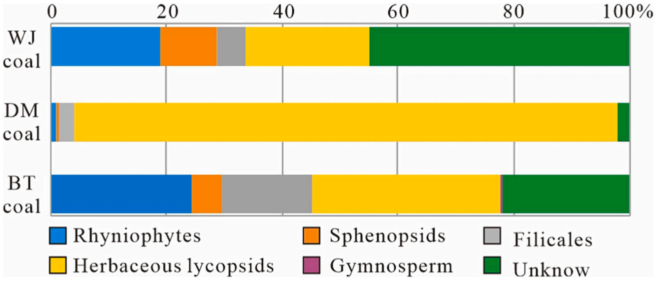

Fig. 14. Distribution of palynomorphs, grouped according to plant affinity in Luquan Devonian coals.

5. Discussion

5.1. Formation of cutinitic liptobioltih

Cutinitic liptobiolith, an unusual coal type, has been discovered in only a few localities worldwide. Its discovery in Siberia dates back to the early 20th century (Lyuber, 1935; Ergolskaya, 1936). Ammosov (1964) reported on the Devonian leaf coal from Germany and the Devonian Barzas coal in South Siberia, noting that these coals contain up to 50 vol % cutinite, originating from the thick cuticles of psilophytes. In the same year, Han (1964) first reported the discovery of Devonian cutinitic liptobiolith in the Luquan region of China, making the Luquan paper coal internationally renowned. Subsequent research revealed that the cutinite content of the Luquan paper coal can be up to 90%, primarily originating from cuticles of vascular plants. In the following decades, this type of coal was reported from few other locations. Volkova (1994) reported the discovery of similar Devonian coals in Kazakhstan and the Timan region, which share similar maceral characteristics with Barzas coal. In addition to the Luquan paper coal, such coal was discovered in the Devonian strata around the Kangdian Uplift in South China, including the Baishaping area of Yunnan Province and the Panzhihua area of Sichuan Province. Song et al. (2017, 2021, 2022b) described a Devonian-age cutinitic liptobiolith from the Bulonggoer area of northwestern China, which was deposited in a freshwater environment and exhibited a sheet-like texture that could be split into leafy laminae.

To the best of our knowledge, nearly all the discovered cutinitic liptobioliths were deposited in the Middle Devonian, especially in the Givetian (Kashirtsev et al., 2010), even though peat accumulation was not extensive during that period. Kennedy et al. (2013) reported cutinite accumulations in Early Devonian carbonaceous materials from northern New Brunswick. However, these materials have a maximum cutinite content of only 27% and cannot be classified as true coals due to their low TOC content (<35.63%) and high ash content (>59.96%, dry basis). Cutinite is also enriched in some Carboniferous coals in Indiana in the USA, the Moscow Basin of Russia, Queensland in Australia, and Thuringia in Germany (Guennel and Neavel, 1959; Neavel and Guennel, 1960; Neavel, 1961; Cook and Taylor, 1963; Auerbach and Trautschold, 1980; Crelling and Bensley, 1980; Kashirtsev et al., 2010; Mousa et al., 2022). However, their cutinite content is <50% vol., so these coals are classified as cutinite-rich coal rather than cutinitic liptobiolith. Late Devonian coals have not been extensively studied. Available data indicate that Late Devonian coals differ from Middle Devonian coals in maceral composition and chemical properties, with well-developed cortex, remains of fructification organs, and no resemblance to Barzas coal (Lapo and Drozdova, 1989). They share similar phyteral composition with Early Carboniferous coals. Consequently, it seems that cuticular liptobioliths were specific for the Middle Devonian, particularly for the Givetian.

Liptobiolith is generally thought to originate from selective decomposition of plant or coaly material, primarily due to oxidation and flowing aqueous medium (Stach et al., 1982; Han et al., 1996). During this process, cellulose, lignin, protein, or their early diagenesis products are completely decomposed and removed from the peatland under aerobic conditions, leaving behind the more resistant cuticles, resins or spores. Mechanical differentiation of plant tissues and selective floating of cuticles can also contribute to the accumulation of cutinite (Tyson, 1995). However, the microscopic characteristics of Luquan Devonian coals, such as the alternation of cutinite and collodetrinite and the low content of inertinite, suggests anoxic peat accumulation conditions with minimal water cover turbulence. In fact, many other cutinitic liptoboilths, including those from the northwestern China, the Panzhihua area of Sichuan Province, and the Baishaping area of Yunnan Province, have also been confirmed to be deposited under similar anoxic peat conditions (Song et al., 2022a, 2022b).

The unique tissue composition of Middle Devonian plants might be responsible for the origin of cutintic liptobiolith during that epoch. The Devonian is considered as one of the most crucial periods on earth for the development of vascular plants (Beerbower et al., 1992; Retallack, 1997; Algeo et al., 2001). During the Late Silurian and Early Devonian, vascular plants remained small and ecologically restricted to moist lowland habitats during this interval (Gray, 1993; Strother et al., 1996). It was not until the Middle Devonian that secondary tissues evolved (i.

e., wood, phloem, and bark with cork), providing the structural support for vascular plants to attain larger sizes and form early forests (Thomas and Spicer, 1987; Beerbower et al., 1992). These earlier land plants commonly had well developed cuticles coating the outer layers of leaves, small roots and stems, for protection against water evaporation and strong ultraviolet radiation. However, the woody tissues of these early plants were less developed, as indicated by the thinner ribbon-like collodetrinite relative to the cutinite in the WJ coals. Under favorable environmental conditions, unique plant assemblages with cuticle-rich foliage were preserved in coals with little vitrinite or other macerals. As vegetation evolved, woody tissue became more prominent in plants, leading to the preservation of greater amounts of vitrinites or inertinites in Late Devonian and younger coals.

5.2. *Molecular composition*

The concentration of tetracyclic diterpenoids in the maltene fraction of coal extracts from WJ, DM and BT sources are 115–130 mg/g, 57–70 mg/g, and 21-24 mg/g, respectively. This data reveals a clear correlation between the levels of tetracyclic diterpenoids and the cutinite content in these coals. Specifically, BT coal extracts, which have the lowest cutinite content, also show the least concentration of tetracyclic diterpenoids. More interestingly, the specific types of cutinite present also significantly influence the abundance of tetracyclic diterpenoids. This is evident in the comparison between WJ and DM coals, both of which have cutinite content over 60%. WJ coals, characterized by a dominance of thick-walled cutinite, have a significantly higher abundance of tetracyclic diterpenoids compared to DM coals, which are primarily composed of medium and thin-walled cutinite. This suggests that thick-walled cutinite may yield more tetracyclic diterpenoids.

Furthermore, the type of cutinite also appears to influence the composition of these diterpenoids. WJ coals display a higher abundance of C_{18}-C_{19} tetracyclic diterpanes compared to their C_{20} homologues. In contrast, DM and BT coals, which predominantly feature medium- and thin-walled cutinite, have a more significant presence of C_{20} compounds. Similar trends have been observed in Bulonggoer, Baishaping and Baras Devonian cutinitic liptobioliths, which are characterized by thick-walled cutinite and a higher amount of C_{18}-C_{19} tetracyclic diterpanes. Conversely, Damaidi cutinitic liptobioliths, dominated by thin-walled cutinite, show a higher abundance of C_{20} diterpanes compared to their C_{18}-C_{19} homologues. Notably, C_{18}-C_{19} tetrayclic diterpanes, having fewer side-chains, are likely to be more matured stable and resistant to biodegradation compared to their C_{20} counterparts.

Tetracyclic diterpenoids are particularly abundant in resins of conifer families, such as Podocarpaceae, Araucariaceae and Cupressaceae families (Hanson, 1972; Bechtel et al., 2022; Otto et al., 2005). Thus, they are believed to be age-related markers of conifers, with their first appearance in the upper Carboniferous linked to the emergence of the earliest conifer (Simoneit, 1977; Schulze and Michaelis, 1990). Since the upper Carboniferous, sedimentary organic matter derived from higher plant sources often contains low concentrations of diterpenoids (Snowdon and Powell, 1982; Philp et al., 1983).

The significant abundance of tetracyclic diterpanes in Devonian cutinite liptobioliths was unexpected because conifers, which are thought to produce these compounds, had not yet evolved during this time. However, all reported Devonian cutinitic liptobioliths contain abundant tetracyclic diterpanes. Sheng et al. (1991, 1992) first reported high abundance of tetracyclic diterpanes in Devonian cutinitic liptobioliths from the Luquan region, China. Subsequently, Cheng et al. (1995), Kashirtsev et al. (2010), and Song et al. (2017, 2022a) found similarly high concentrations of these compounds in Devonian cutinitic liptobioliths from various locations, including Huaping (Yunnan Province), Panzhihua (Sichuan Province), and Bulonnggoer regions of China, as well as Russia. The abundant presence of tetracyclic diterpanes in Devonian cutinitic liptobioliths suggest that the biosynthesis of these tetracyclic diterpenoids, with beyerane, atisane and kaurane skeletons, had already evolved in early land plants. Although massive tetracyclic diterpanes were found in cutinitic liptobiolith, they are either absent or present in low abundance in other types of coals or shales from the middle Devonian with little contribution of cutinite (Fowler et al., 1991; Song et al., 2017). This indicates that the precursor of these compounds might be important components of early land plant cuticles or at least coexist alongside plant cuticles.

6. Conclusion

The Middle Devonian coals in the Luquan region of China are internationally renowned for their high content of cutinite. These coals, classified as cutinitic liptobioliths, are often referred to as “paper coal” due to their distinctive papery texture. However, notable differences exist in the macroscopic, microscopic, and geochemical features of coal samples collected from the WJ, DM and BT areas within the Luquan region. The coal-forming plants of these cutinitic liptobioliths were primarily herbaceous lycopsids, rhyniopsids, *Orestovia* and *Spongiophyton*, but the specific types varied by area, leading to the unique macroscopic and microscopic characteristics observed in coals from different locations.

Abundant tetracyclic diterpenoids were detected in extracts from all the Luquan Middle Devonian coal samples. The concentration and composition of these diterpenoids vary depending on the content and type of cutinite in the coals. Remarkably, tetracyclic diterpenoids have been identified in considerable amounts in Middle Devonian cutinitic liptobioliths worldwide. Their widespread presence indicates that the biosynthesis of these tetracyclic diterpenoids had already evolved in early land plants. Furthermore, it is likely that the precursors of these compounds were important components of early land plant cuticles, or at the very least, they coexisted alongside plant cuticles.

CRediT authorship contribution statement

Daofu Song: Conceptualization, Methodology, Investigation, Writing – original draft. **Tieguan Wang:** Methodology, Writing – review & editing. **Hao Wang:** Visualization, Investigation. **Honghe Xu:** Methodology, Writing – original draft. **Zhengang Lu:** Visualization. **Yue Liu:** Visualization.

Declaration of competing interest

The authors declare that they have no known competing financial interests or personal relationships that could have appeared to influence the work reported in this paper.

Data availability

Data will be made available on request.

Acknowledgement

This study was founded by the National Natural Science Foundation of China (Grant No. 42273029 and 42073069).

References

Algeo, T.J., Scheckler, S.E., Maynard, J.B., 2001. Effects of the Middle to Late Devonian spread of vascular land plants on weathering regimes, marine biota, and global climate. In: Gensel, P.G., Edwards, D. (Eds.), Plants Invade the Land: Evolutionary and Environmental Perspectives. Columbia University Pres, New York, pp. 213–236.

Ammosov, I.I., 1964. Composition pétrographique des charbons humiques de l'USSR. Congr. Intern. Strat. Geol. Carboniférе 3, 909–916.

ASTM Standard D2798-11a, 2019. Test Method for Microscopical Determination of the Vitrinite Reflectance of Coal. ASTM International, West Conshohocken, PA.

ASTM Standard D3173, 2011. Test Method for Moisture in the Analysis Sample of Coal and Coke. ASTM International, West Conshohocken, PA.

ASTM Standard D3174, 2011. Annual Book of ASTM Standards. Test Method for Ash in the Analysis Sample of Coal and Coke. ASTM International, West Conshohocken, PA.

ASTM Standard D3175, 2011. Test Method for Volatile Matter in the Analysis Sample of Coal and Coke. ASTM International, West Conshohocken, PA.

ASTM Standard D3177–02, 2011. Test Methods for Total Sulfur in the Analysis Sample of Coal and Coke. (Reapproved 2007). ASTM International, West Conshohocken, PA.

ASTM Standard D388, 2018. Standard Classification of Coals by Rank. ASTM International, West Conshohocken, PA.

Auerbach, J., Trautschold, H., 1980. Ueber die Kohlen von Central-Russland. Soc. Naturalistes Moscou. Nouv. Mem. 13, 1–58.

Balme, B.E., 1995. Fossil in situ spores and pollen grains: an annotated catalogue. Rev. Palaeobot. Palynol. 87, 81–323.

Bechtel, A., Sachsenhofer, R.F., Gratzer, R., Lücke, A., Püttmann, W., 2022. Parameters determining the carbon isotopic composition of coal and fossil wood in the Early Miocene Oberdorf lignite seam (Styrian Basin, Austria). Org. Geochem. 33, 1001–1024.

Beerbower, J.R., Boy, J.A., DiMichele, W.A., Gastaldo, R.A., Hook, R., Hotton, I.I.I.N., Phillips, T.L., Scheckler, S.E., Shear, W.A., 1992. Paleozoic terrestrial ecosystems. In: Behrensmeyer, A.K., Damuth, J.D., DiMichele, W.A., Potts, R., Sues, H.D., Wing, S.L. (Eds.), Terrestrial Ecosystems through Time. University Chicago Press, Chicago, pp. 205–235.

Cheng, D.S., Han, D.X., Wang, Y.B., Xiao, X.M., Sheng, G.Y., 1995. Coal petrological study of China Devonian coal. Coal. Geol. Explor. 23 (1), 25–28.

Cook, A.C., Taylor, G.H., 1963. The petrography of some Triassic Ipswich coals. Australas Inst. Min. Met. Proc. 205, 35–55.

Crelling, J.C., Bensley, D.F., 1980. Petrology of cutinite-rich coal from the Roaring Creek Mine area Parke County, Indiana. In: Langenheim, R.L., Mann, C.J. (Eds.), Middle and Late Pennsylvanian Strata on Margin of Illinois Basin. Soc Econ Paleontol Mineral 10th Annu Field Conf Guidebook, pp. 93–104.

Dai, S.F., Han, D.X., Chou, C.L., 2006. Petrography and geochemistry of the Middle Devonian coal from Luquan, Yunnan Province, China. Fuel 85, 456–464.

Diessel, C.F., 2010. The stratigraphic distribution of inertinite. Int. J. Coal Geol. 81, 251–268.

Ergolskaya, Z.V., 1936. Petrographic Study of Barzas Coals. ONTI, Moscow.

Evenick, J.C., 2021. Examining the relationship between T_{max} and vitrinite reflectance: an empirical comparison between thermal maturity indicators. J. Nat. Gas Sci. Eng. 9, 1–8.

Fang, R.S., 2000. A discussion about the Devonian stratigraphy of Yunnan. Yunnan Geol. 19 (1), 62–90.

Fletcher, B.J., Beerling, D.J., Chaloner, W.G., 2004. Stable carbon isotopes and the metabolism of the terrestrial Devonian organism *Spongiophyton*. Geobiol 2, 107–119.

Fowler, M.G., Goodarzi, F., Gentzis, T., Brocks, P.W., 1991. Hydrocarbon potential of Middle and Upper Devonian coals from Melville Island, Arctic Canada. Org. Geochem. 17, 681–694.

Gensel, P.G., Chaloner, W.G., Forbes, W.H., 1991. *Spongiophyton* from the late Lower Devonian of New Brunswick and Quebec, Canada. Palaeontol 34, 149–168.

Gray, J., 1993. Major Paleozoic land plant evolutionary bio-events. Palaeogeogr. Palaeoclimatol. Palaeoecol. 104, 153–169.

Guennel, G.K., Neavel, R.C., 1959. Paper coal in Indiana. Science 129, 1671–1672.

Guo, Y., Wang, D.M., 2016. Studies on plant cuticle from the Lower-Middle Devonian of China. Rev. Palaeobot. Palynol. 227, 42–51.

Han, D.X., 1964. Preliminary study on the petrology of the Devonian liptobioliths in Luquan, Yunnan. J. China Soc. 1, 95–99.

Han, D.X., 1989. The features of Devonian coal-bearing deposits in South China, the People's Republic of China. Int. J. Coal Geol. 12, 209–233.

Han, D.X., Wang, Y.B., Quan, B., Cheng, D.S., 1993. The evolution of Devonian coal accumulation in China. Coal. Geol. Explor. 21 (5), 1–6.

Han, D.X., Ren, D.Y., Wang, Y.B., Jin, K.L., Mao, H.L., Qin, Y., 1996. Coal Petrology of China. China University of Mining and Technology Press, Xuzhou.

Hanson, J.R., 1972. The di- and sesterterpenes – Part I. In: Newman, A.A. (Ed.), Chemistry of Terpenes and Terpenoids. Academic Press, London, pp. 155–199.

International Committee for Coal and Organic Petrology (ICCP), 1998. The new vitrinite classification (ICCP system 1994). Fuel 77, 349–358.

International Committee for Coal and Organic Petrology (ICCP), 2001. New inertinite classification (ICCP system 1994). Fuel 80, 459–471.

ISO 11760, 2005. Classification of Coals, 1st edition. International Organization for Standardization, Geneva, Switzerland, p. 9.

Jahren, A.H., Porter, S., Kuglitsch, J.J., 2003. Lichen metabolism identified in Early Devonian terrestrial organisms. Geol 31, 99–102.

Kalkreuth, W.D., 1982. Rank and petrographic composition of selected Jurassic-Lower cretaceous coals of British Columbia, Canada. Bull. Can. Petrol. Geol. 30 (2), 112–139.

Kashirtsev, V.A., Moskvin, V.I., Fomin, A.N., Chalaya, O.N., 2010. Terpanes and steranes in coals of different genetic types in Siberia. Russ. Geol. Geophys. 51, 404–411.

Kennedy, K.L., Gibling, M.R., Eble, C.F., Gastaldo, R.A., Gensel, P.G., Werner-Zwanziger, U., Wilson, R.A., 2013. Lower Devonian Coaly shales of Northern New Brunswick, Canada: plant accumulations in the early stages of terrestrial colonization. J. Sediment. Res. 83, 1202–1215.

Krassilov, V., 1981. *Orestovia* and the origin of vascular plants. Lethaia 44, 235–250.

Lapo, A.V., Drozdova, I.N., 1989. Phyterals of humic coals in the U.S.S.R. Int. J. Coal Geol. 12, 477–510.

Lyuber, A.A., 1935. The Barzas-Type Coal in Southeastern Kazakhstan. Khim. Tverd Topliva 6 (1), 14–17.

Marshall, J.E.A., Zhu, H.C., Wellman, C.H., Berry, C.M., Wang, Y., Xu, H.H., Breuer, P., 2017. Provincial Devonian spores from South China, Saudi Arabia and Australia. Rev. Micropaleontol. 60, 403–409.

Mei, B.W., Wang, T.G., Liu, H.R., Chen, K.Q., 1989. Tetracyclic diterpanes of Carboniferous and Permian humic coals in North China. Acta Sedimentol. Sin. 7 (4), 133–140.

Moroeng, O.M., Wagner, N.J., Brand, D.J., Roberts, R.J., 2018. A nuclear magnetic resonance study: implications for coal formation in the Witbank Coalfield, South Africa. Int. J. Coal Geol. 188, 145–155.

Mousa, D.A., Makled, W.A., Gentzis, T., Gad, N.S., Samaan, J., 2022. Discovery of an extraordinary Carboniferous cutinite-rich coal seam from Wadi Abu Thora, southern Sinai, Egypt: Organic petrographical and geochemical characterization. Int. J. Coal Geol. 250, 103908.

Mukhopadhyay, P.K., Hatcher, P.G., Calder, J.H., 1991. Hydrocarbon generation from deltaic and intermontane fluviodeltaic coal and coaly shale from the Tertiary of Texas and Carboniferous of Nova Scotia. Org. Geochem. 17, 765–783.

Neavel, R.C., 1961. Petrographic and chemical composition of Indiana coals. Indiana Geol. Survey Bull. 22, 81.

Neavel, R.C., Guennel, G.K., 1960. Indiana paper coal: Composition and deposition. SEPM J. Sediment Res. 30, 241–248.

Noble, R., Knox, J., Alexander, R., Kagi, R., 1985. Identification of tetracyclic diterpene hydrocarbons in Australian crude oils and sediments. J. Chem. Soc. Chem. Commun. 1, 32–33.

Noble, R., Alexander, R., Kagi, R.I., Nox, J.K., 1986. Identification of some diterpenoid hydrocarbons in petroleum. Org. Geochem. 10, 825–829.

Otto, A., Simoneit, B.R.T., Rember, W.C., 2005. Conifer and angiosperm biomarkers in clay sediments and fossil plants from the Miocene Clarkia Formation, Idaho, USA. Org. Geochem. 36, 907–922.

Peters, K.E., Moldowan, J.M., 1993. The Biomarker Guide: Interpreting Molecular Fossils in Petroleum and Ancient Sediments. Prentice Hall, Englewood Cliffs, NJ.

Peters, K.E., Walters, C.C., Moldowan, J.M., 2005. The Biomarker Guide, Second Edition. Cambridge University Press, UK.

Peterson, H.I., Vosgeran, H., 1999. Composition and organic maturity of middle Jurassic coal, North-East Greenland: evidence for liptinite-induced suppression of huminite reflectance. Int. J. Coal Geol. 41, 257–274.

Philp, R.P., Simoneit, B.R.T., Gilbert, T.D., 1983. Diterpenoids in crude oils and coals of South Eastern Australia. In: Bjoroy, M. (Ed.), Advances in Organic Geochemistry 1981. Wiley, Chichester, pp. 698–704.

Pickel, W., Kus, J., Flores, D., 2017. Classification of liptinite-ICCP System 1994. Int. J. Coal Geol. 169, 40–61.

Powell, T.G., McKirdy, D.M., 1973. Relationship between ratio of pristane to phytane, crude oil composition and geological environment in Australia. Nat. Phys. Sci. 243, 37–39.

Retallack, G.J., 1997. Early forest soils and their role in Devonian global change. Science 276, 583–585.

Schulze, T., Michaelis, W., 1990. Structure and origin of terpenoid hydrocarbons in some German coals. Org. Geochem. 16, 1051–1058.

Scot, A.C., Glasspool, I.J., 2007. Observations and experiments on the origin and formation of inertinite group macerals. Int. J. Coal Geol. 70, 53–66.

Sheng, G.Y., Fu, J.M., Liu, D.H., Chen, X.J., Simoneit, B.R.T., Han, D.X., 1991. Tetracyclic diterpanes enriched in Devonian cutinite coal. Oil Gas Geol. 12 (2), 107–116.

Sheng, G.Y., Simoneit, B.R.T., Leif, R.N., Chen, X., Fu, J., 1992. Tetracyclic terpanes enriched in Devonian cuticle humic coals. Fuel 71, 523–532.

Simoneit, B.R.T., 1977. Diterpenoid compounds and other lipids in deep-sea sediments and their geochemical significance. Geochim. Cosmochim. Acta 41, 463–476.

Snowdon, L.R., Powell, T.G., 1982. Immature oil and condensate-modification of hydrocarbon generation model for terrestrial organic matter. AAPG Bull. 66, 775–788.

Song, D.F., Simoneit, B.R.T., He, D.F., 2017. Abundant tetracyclic terpenoids in a Middle Devonian foliated cuticular liptobiolite coal from northwestern China. Org. Geochem. 107, 9–20.

Song, D.F., Wang, T.G., Zhong, N.N., Chen, Y., He, D.F., 2021. Discovery of cutinitic liptobiolith in northwestern China and a comparative study with Luquan Devonian coal. Sci. China Earth Sci. 64 (4), 642–650.

Song, D.F., Wang, T.G., Li, P., Zhang, M., He, D.F., 2022a. Petrology and geochemistry of Devonian cutinitic liptobioliths from northwestern China. Int. J. Coal Geol. 253, 1–16.

Song, D.F., Wang, T.G., Li, P., Zhang, M., Liu, A.L., Yan, J.D., 2022b. Petrology and organic geochemistry of the Baishaping and Damaidi Devonian cutinitic liptobioliths, west of the Kangdian Uplift, China. Pet. Sci. 19, 1978–1992.

Stach, E., Taylor, G.H., Mackowsky, M.T., Chandra, D., Teichmüller, M., Teichmüller, R., 1982. Stach's Textbook of Coal Petrology. Gebrüder Borntråger, Berlin.

Stein, W.E., Harmon, G.D., Hueber, F.M., 1993. *Spongiophyton* from the Lower Devonian of North America reinterpreted as a lichen. Am. J. Bot. 80, 93.

Strother, P.K., Al-Hajri, S., Traverse, A., 1996. New evidence for land plants from the lower Middle Ordovician of Saudi Arabia. Geol 24, 55–58.

Teichmiiller, M., 1974. Uber neue macerale der liptinit-gruppe und die entstehung des micrinits. Fortschr. Geol. Rheinld. Westf. 24, 37–64.

Teichmtiller, M., 1974. Entstehung und veranderung bituminoser substanzen in Kohlen in Beziehung zur Entstehung und Umwandlang tier Erdols. Fortschr. Geol. Rheinld. Westf. 24, 65–112.

Thomas, B.A., Spicer, R.A., 1987. The Evolution and Palaeobiology of Land Plants. Croom Helm, London.

Tissot, B.P., Welte, D.H., 1984. Petroleum Formation and Occurrence-a New Approach to Oil and Gas Exploration. Springer-Verlag, Berlin.

Tyson, R.V., 1995. Sedimentary Organic Matter-Organic Facies and Palynofacies. Chapman and Hall, Devon.

Van Krevelen, D.W., 1961. Coal. Elsevier, Amsterdam.

Volkova, I.B., 1994. Nature and composition of the Devonian coals of Russia. Energy Fuel 8, 1489–1493.

Wang, Y., Berry, C.M., Hao, S.G., Xu, H.H., Fu, Q., 2007. The Xichong flora of Yunnan, China: diversity in late Mid Devonian plant assemblages. Geol. J. 42, 339–350.

Zinniker, D.A., 2005. New Insights into Molecular Fossils: The Fate of Terpenoids and the Origin of Gem-Dialkylalkanes in the Geological Environment.. Ph.D. thesis Stanford University.